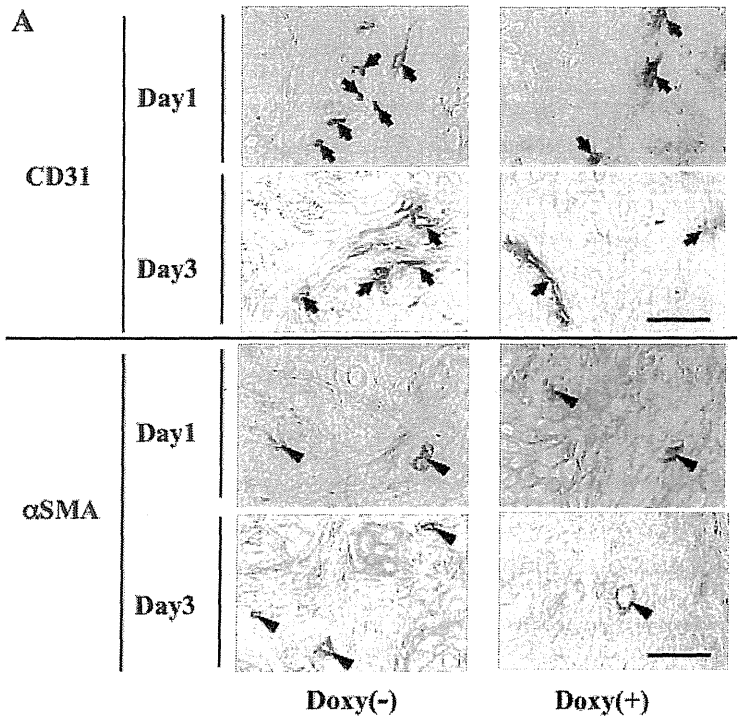

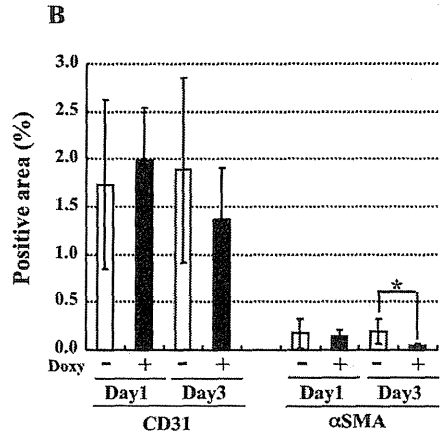

Fig. 4 Immunohistochemically stained tumor xenografts from control (Doxy –) and doxycycline treated (Doxy +) mice. (A) Frozen tumor tissue sections were stained with anti-CD31 (endothelial cell marker) antibody or anti-*α* smooth muscle actin (smooth muscle cell marker, αSMA) antibody. Large vascular structures were prominent in tumor xenografts from doxycycline non-treated animals. Arrows indicate endothelial cells positive for CD31 and arrowheads indicate vascular vessels positive for *α* smooth muscle actin. Bars indicate 100 μm. (B) Areas positively stained with anti-CD31 or anti-*α* smooth muscle actin (αSMA) were measured on 5 randomly chosen visual fields at 200 times magnifications. *: $P < 0.05$ as indicated by the bracket.

Immunohistochemical studies

In order to clarify the reason for the suppression of the tumor growth in the BRA/CXCL14-expressing cells under the *in vivo*, but not under the *in vitro* situation, we examined the infiltration of blood vessels into the tumor tissue. When vascular endothelial cells in the tumor were immunohistochemically stained with anti-CD31 antibody, the number of CD31-positive endothelial cells at 1 day and 3 days after the xenografting was the same whether or not the tumor-bearing mice had been treated with doxycycline (Fig. 4A and B). However, when the sections were stained with anti-α smooth muscle actin antibody, a marker for smooth muscle cells, the area of positive staining surrounding the endothelial cells was significantly smaller in tumors 3 days after treatment with doxycycline (Fig. 4A and B).

DISCUSSION

In HNSCC cells, including HSC-2 cells, the expression of BRAK/CXCL14 is down-regulated. The expression is negatively regulated by the binding of epidermal growth factor (EGF) to its receptor (16); and when HNSCC cells are treated with gefitinib, an epidermal growth factor tyrosine kinase inhibitor, the expression of BRAK/CXCL14 protein increases under culture conditions (15). Interestingly, the oral administration of gefitinib significantly ($P < 0.001$) reduces the growth of tumor xenografts of 3 HNSCC cell lines (HSC-2, HSC-3 and HSC-4) in female athymic nude mice, which reduction is accompanied by an increase in BRAK expression specifically in the tumor tissue; this tumor-suppressing effect of the drug is not observed in the case of BRAK non-expressing cells (15). Furthermore, the introduction of a vector expressing short hairpin RNA against BRAK reduces both the expression level of BRAK/CXCL14 in HSC-3 cells and the antitumor efficacy of gefitinib *in vivo* (15). These data indicate an inverse relationship between BRAK expression levels in tumor cells and the tumor growth

rate.

Here we showed that the expression of BRAK/CXCL14 protein induced in tumor cells by treatment with doxycycline *in vivo* resulted in significant reduction in the size of tumors compared with the size of the control mice (Fig. 3A and B), even though expression of the protein under culture conditions did not affect the rate of growth of the cells (Fig. 2A and B). The results obtained here indicate that the expression of BRAK/CXCL14 itself without the co-presence of gefitinib is sufficient to reduce the growth rate of tumors *in vivo*.

The present data showed significant down-regulation of the size of tumors shortly after tumor-cell xenografting when doxycycline-pretreated tumor cells were used and the host mice had been also pretreated with the drug before tumor cell xenografting. These results indicate that tumor cell settlement in the host tissues was also suppressed by the expression of BRAK/CXCL14 in the tumor cells.

In order to investigate further the effect of BRAK/CXCL14 expression on tumor formation, we stained the tumor tissues in the xenografted mice with anti-CD31 antibody, a marker for vascular endothelial cells. We could not find any significant difference between doxycycline-treated and un-treated animals in terms of staining intensity (Fig. 4A and B). However, a significant difference in the area positive for α smooth muscle actin was observed between tumors of doxycycline-treated and un-treated animals 3 days after injection of tumors (Fig. 4A and B). It is reported that recombinant BRAK/CXCL14 inhibits *in vivo* angiogenesis induced by IL-8 (CXCL8), basic FGF or VEGF and that binding of BRAK/CXCL14 to human umbilical vein endothelial cells and human dermal micro-vascular endothelial cells is not detectable (23). Recently it was clarified that tumor blood vessels are atypical and immature, and they have poorly developed vessel walls that are invested inadequately with vascular smooth muscle cells (4, 10). Our data coincide well with these reports and suggest the possibility that the target cell of BRAK/CXCL14 is the smooth muscle cell and not the vascular endothelial cell and that BRAK/CXCL14 inhibits the proliferation and/or chemotaxis-directed movement of smooth muscle cells, which is essential for maturation of blood vessels. Thus, such inhibition would restrain the formation of functional vessels and consequently inhibit growth of tumors.

In conclusion we showed, using Tet-on BRAK HSC-2 cells that expressed BRAK/CXCL14 protein under regulation of doxycycline, inhibition of both the settlement and proliferation of tumor cells *in vivo*, even though expression of the chemokine did not affect growth properties of the tumor cells *in vitro*. Furthermore, the suppression of the tumor growth *in vivo* was found to be at least dependent on the inhibition of maturation of tumor blood vessels. Our present findings may be useful for the clarification of the molecular mechanisms of BRAK/CXCL14 functions *in vivo*.

Acknowledgements

We thank Dr. H. Miyoshi (RIKEN) for providing lentivirus vectors and packaging constructs. We also appreciate Dr. Yasumasa Kato for valuable discussion and Ms. Etsuko Shimada for preparation of the reference list. A part of this work was performed at the Oral Health Science Research Center, Kanagawa Dental College and supported by a Grant-in Aid from the High-Tech Research Center Project of the Ministry of Education, Culture, Sports, Science and Technology of Japan (S.I., S.O, and R.H.) and by Scientific Research, Japan Society for Promotion of Sciences (R.H.). Another part of the work was performed at National Cancer Center Research Institute and supported by a Grant-in-Aid from the Ministry of Health, Labor and Welfare of Japan (T.K.).

REFERENCES

1. Allinen M, Beroukhim R, Cai L, Brennan C, Lahti-Domenici J, Huang H, Porter D, Hu M, Chin L, Richardson A, Schnitt S, Sellers WR and Polyak K (2004) Molecular characterization of the tumor microenvironment in breast cancer. *Cancer Cell* **6**, 17–32.
2. Balkwill F (2004) Cancer and the chemokine network. *Nat Rev Cancer* **4**, 540–550.
3. Castellanos A, Vicente-Duenas C, Campos-Sanchez E, Cruz JJ, Garcia-Criado FJ, Garcia-Cenador MB, Lazo PA, Perez-Losada J and Sanchez-Garcia I (2010) Cancer as a reprogramming-like disease: Implications in tumor development and treatment. *Semin Cancer Biol*, Feb 24 [Epub ahead of print].
4. Dudley AC, Khan ZA, Shih SC, Kang SY, Zwaans BM, Bischoff J and Klagsbrun M (2008) Calcification of multipotent prostate tumor endothelium. *Cancer Cell* **14**, 201–211.
5. Emery DW, Yannaki E, Tubb J and Stamatoyannopoulos G (2000) A chromatin insulator protects retrovirus vectors from chromosomal position effects. *Proc Natl Acad Sci USA* **97**, 9150–9155.
6. Frederick MJ, Henderson Y, Xu X, Deavers MT, Sahin AA, Wu H, Lewis DE, El-Naggar AK and Clayman GL (2000) In vivo expression of the novel CXC chemokine BRAK in normal and cancerous human tissue. *Am J Pathol* **156**, 1937–1950.
7. Hossini AM, Eberle J, Fecker LF, Orfanos CE and Geilen CC (2003) Conditional expression of exogenous Bcl-X(S)

triggers apoptosis in human melanoma cells in vitro and delays growth of melanoma xenografts. *FEBS Lett* **553**, 250–256.
8. Hromas R, Broxmeyer HE, Kim C, Nakshatri H, Christopherson K, 2nd, Azam M and Hou YH (1999) Cloning of BRAK, a novel divergent CXC chemokine preferentially expressed in normal versus malignant cells. *Biochem Biophys Res Commun* **255**, 703–706.
9. Koch U, Krause M and Baumann M (2010) Cancer stem cells at the crossroads of current cancer therapy failures-radiation oncology perspective. *Semin Cancer Biol*, Feb 26 [Epub ahead of print].
10. McKeage MJ and Baguley BC (2010) Disrupting established tumor blood vessels: an emerging therapeutic strategy for cancer. *Cancer* **116**, 1859–1871.
11. McKinnon CM, Lygoe KA, Skelton L, Mitter R and Mellor H (2008) The atypical Rho GTPase RhoBTB2 is required for expression of the chemokine CXCL14 in normal and cancerous epithelial cells. *Oncogene* **27**, 6856–6865.
12. Miyoshi H (2004) Gene delivery to hematopoietic stem cells using lentiviral vectors. *Methods Mol Biol* **246**, 429–438.
13. Naviaux RK, Costanzi E, Haas M and Verma I MV (1996) The pCL vector system: rapid production of helper-free, high-titer, recombinant retroviruses. *J Virol* **70**, 5701–5705.
14. O'Brien CA, Pollett A, Gallinger S and Dick JE (2007) A human colon cancer cell capable of initiating tumour growth in immunodeficient mice. *Nature* **445**, 106–110.
15. Ozawa S, Kato Y, Ito S, Komori R, Shiiki N, Tsukinoki K, Ozono S, Maehata Y, Taguchi T, Imagawa-Ishiguro Y, Tsukuda M, Kubota E and Hata RI (2009) Restoration of BRAK/CXCL14 gene expression by gefitinib is associated with antitumor efficacy of the drug in head and neck squamous cell carcinoma. *Cancer Sci* **100**, 2202–2209.
16. Ozawa S, Kato Y, Komori R, Maehata Y, Kubota E and Hata R (2006) BRAK/CXCL14 expression suppresses tumor growth *in vivo* in human oral carcinoma cells. *Biochem Biophys Res Commun* **348**, 406–412.
17. Ozawa S, Kato Y, Kubota E and Hata R (2009) BRAK/CXCL14 expression in oral carcinoma cells completely suppresses tumor cell xenografts in SCID mouse. *Biomed Res* **30**, 315–318.
18. Ricci-Vitiani L, Lombardi DG, Pilozzi E, Biffoni M, Todaro M, Peschle C and De Maria R (2007) Identification and expansion of human colon-cancer-initiating cells. *Nature* **445**, 111–115.
19. Rollins BJ (2006) Inflammatory chemokines in cancer growth and progression. *Eur J Cancer* **42**, 760–767.
20. Sasaki R, Narisawa-Saito M, Yugawa T, Fujita M, Tashiro H, Katabuchi H, and Kiyono T (2009) Oncogenic transformation of human ovarian surface epithelial cells with defined cellular oncogenes. *Carcinogenesis* **30**, 423–431.
21. Sato K, Ozawa S, Izukuri K, Kato Y and Hata RI (2010) Expression of tumor-suppressing chemokine BRAK/CXCL14 reduces cell migration rate of HSC-3 tongue carcinoma cells and stimulates attachment to collagen and formation of elongated focal adhesions in vitro. *Cell Biol Int*, **34**, 513–522.
22. Schwarze SR, Luo J, Isaacs WB and Jarrard DF (2005) Modulation of CXCL14 (BRAK) expression in prostate cancer. *Prostate* **64**, 67–74.
23. Shellenberger TD, Wang M, Gujrati M, Jayakumar A, Strieter RM, Burdick MD, Ioannides CG, Efferson CL, El-Naggar AK, Roberts D, Clayman GL and Frederick MJ (2004) BRAK/CXCL14 is a potent inhibitor of angiogenesis and a chemotactic factor for immature dendritic cells. *Cancer Res* **64**, 8262–8270.
24. Shockett P, Difilippantonio M, Hellman N and Schatz DG (1995) A modified tetracycline-regulated system provides autoregulatory, inducible gene expression in cultured cells and transgenic mice. *Proc Natl Acad Sci USA* **92**, 6522–6526.
25. Shurin GV, Ferris RL, Tourkova IL, Perez L, Lokshin A, Balkir L, Collins B, Chatta GS and Shurin MR (2005) Loss of new chemokine CXCL14 in tumor tissue is associated with low infiltration by dendritic cells (DC), while restoration of human CXCL14 expression in tumor cells causes attraction of DC both in vitro and in vivo. *J Immunol* **174**, 5490–5498.
26. Sleeman MA, Fraser JK, Murison JG, Kelly SL, Prestidge RL, Palmer DJ, Watson JD and Kumble KD (2000) B cell- and monocyte-activating chemokine (BMAC), a novel non-ELR α-chemokine. *Int Immunol* **12**, 677–689.
27. Suzuki K, Oida T, Hamada H, Hitotsumatsu O, Watanabe M, Hibi T, Yamamoto H, Kubota E, Kaminogawa S and Ishikawa H (2000) Gut cryptopatches: Direct evidence of extrathymic anatomical sites for intestinal T lymphopoiesis. *Immunity* **13**, 691–702.
28. Wente MN, Mayer C, Gaida MM, Michalski CW, Giese T, Bergmann F, Giese NA, Büchler MW and Friess H (2008) CXCL14 expression and potential function in pancreatic cancer. *Cancer Lett* **259**, 209–217.
29. Zlotnik A (2006) Chemokines and cancer. *Int J Cancer* **119**, 2026–2029.
30. Zlotnik A and Yoshie O (2000) Chemokines: a new classification system and their role in immunity. *Immunity* **12**, 121–127.

Cancer Science
The official journal of the Japanese Cancer Association JCA

Prevalence of human papillomavirus 16/18/33 infection and p53 mutation in lung adenocarcinoma

Reika Iwakawa,[1] Takashi Kohno,[1] Masato Enari,[1] Tohru Kiyono[2] and Jun Yokota[1,3]

Divisions of [1]Biology and [2]Virology, National Cancer Center Research Institute, Tokyo, Japan

(Received March 11, 2010/Revised April 28, 2010/Accepted April 30, 2010/Accepted manuscript online May 19, 2010/Article first published online June 14, 2010)

Human papillomavirus (HPV) infection is a causative event for the development of uterine cervical carcinoma. Human papillomavirus (HPV) 16, 18, and 33 DNA has been also detected frequently in lung adenocarcinomas (AdCs) in East Asian countries; however, its prevalence in Japan remains unclear. We therefore screened for HPV 16/18/33 DNA in 297 lung AdCs in a Japanese population by multiplex PCR with type-specific primers. As reported previously, HPV 16 DNA was detected in two cervical cancer cell lines, CaSki and SiHa, while HPV 18 DNA was detected in HeLa cells, and 0.1–1.0 copies of HPV-DNA per cell were detectable by this method. However, with this method, none of the 297 lung AdCs showed positive signals for HPV 16/18/33 DNA, indicating that HPV-DNA is not or is very rarely integrated in lung AdC genomes in the Japanese. Furthermore, none of the lung AdCs showed positive signals by nested PCR with HPV 16/18 type-specific primers. Therefore, we further attempted to detect HPV 16/18/33 DNA in 91 lung cancer cell lines, including 40 AdC cell lines. Among them, 30 have been established in Japan and the remaining 61 in the USA. No HPV signals were obtained in any of the 91 cell lines by either multiplex or nested PCR, while the *p53* gene was mutated in 81 of them including 35 of the 40 AdC cell lines. These results indicate that HPV 16/18/33 infection does not play a major role in the development of lung AdC in Japan nor in the USA. (*Cancer Sci* 2010; 101: 1891–1896)

Infection with human papillomavirus (HPV) is a critical event for the development of uterine cervical cancer.[1] E6 protein, encoded by HPV, binds the host cellular tumor suppressor protein p53, and triggers its degradation through the ubiquitin pathway.[2,3] Therefore, the biological significance of continuous p53 degradation by HPV-E6 protein in cervical carcinoma is thought to be equivalent to that of p53 inactivation by genetic alterations in various other types of cancers in human carcinogenesis. The *p53* gene is frequently inactivated in lung adenocarcinoma (AdC) by mutations and/or deletions of both alleles, and the prevalence of p53 mutations in lung AdC is approximately 50% with a higher incidence in smokers.[4,5] However, p53 is not genetically altered in the other half of lung AdCs. Therefore, it is possible that p53 is inactivated by other mechanisms in lung AdC cells without p53 mutations. For this reason, there have been many reports investigating the involvement of HPV in lung AdC development. However, the prevalence of HPV infection in lung AdCs varies drastically among the reports.[5–7] Recently, reasons for a wide variation in the prevalence of HPV infection in lung cancer were investigated by two systematic surveys of a large number of publications.[6,7] A higher prevalence in Asia than in Europe was pointed out by these two investigations,[6,7] and a higher prevalence in studies using HPV type-specific primers than in those using consensus HPV primers was also pointed out in the latter investigation.[7] In East Asia (Supplementary Table S1), a high incidence of HPV infection in lung AdC was reported from Taiwan (92.8%), China (46.9%), and Korea (55.1%).[8–10] In particular, a high prevalence of HPV 16 and 18 infections was reported from Taiwan and China and of HPV 33 infection from Korea. In Japan, the incidence of HPV infection (0–19.4%) has been reported to be not as high as in other East Asian countries, but is still high enough to consider its involvement in lung AdC development.[11–14]

Taiwan, China, and Korea are geographically close to Japan and the people in these countries are ethnically also close to the Japanese. Therefore, in this study, we aimed to elucidate whether or not HPV 16, 18, and 33 are also involved in the development of lung AdC in Japan, as in Taiwan, China, and Korea. We applied a multiplex PCR method as well as a nested PCR method using type-specific primers for detection of HPV 16, 18, and 33 DNA in 275 primary and 22 metastatic lung AdCs in Japanese, and also in 91 lung cancer cell lines established in either Japan or the USA. To validate the specificity and sensitivity of HPV detection methods, three cervical carcinoma cell lines were analyzed by the same methods. In 91 cell lines, the status of p53 mutations was comprehensively analyzed and the results were compared with several p53 databases to evaluate accurately the prevalence of p53 inactivation in lung cancers.

Materials and Methods

Patients and tissues. A total of 275 primary lung AdCs and 22 metastatic lung AdCs to the brain were obtained at surgery from patients treated at the National Cancer Center Hospital, Tokyo, and at Saitama Medical University Hospital. The tumors were pathologically diagnosed according to the tumor-node-metastasis classification of malignant tumors[15] (Table 1). Tumor tissues were stored at –80°C until DNA extraction, and genomic DNA was extracted as previously described.[16] This study was undertaken under the approval of the Institutional Review Board of the National Cancer Center.

Cell line DNA. DNA from 91 lung cancer cell lines[17,18] was screened for HPV-DNA in its genome. These cell lines consisted of 40 AdCs, 11 squamous cell carcinomas (SqCs), two adenosquamous carcinomas (ASCs), nine large-cell carcinomas (LCCs), 27 small-cell lung carcinomas (SCLCs), and two others (one carcinoid tumor and one neuroendocrine tumor), as listed in Table 2. Detailed information will be provided upon request. DNA from three cervical carcinoma cell lines, CaSki, SiHa, and HeLa, and HPV 33 containing plasmid DNA, was used as positive controls for detection of HPV-DNA.

Multiplex PCR with HPV type-specific primers. Sequences for the E1 and L2 regions of HPV 16 and for the E1 region of HPV 18 and 33, together with the aminolevulinate, delta-, synthase 1 (ALAS1) gene segment as an internal positive control, were simultaneously amplified by multiplex PCR in a single tube, as reported.[19] The primer sequences are shown in Supplementary Table S2. Multiplex PCR was performed with Takara Taq (Takara, Shiga, Japan) with a volume of 50 μL containing 1×

[3]To whom correspondence should be addressed.
E-mail: jyokota@ncc.go.jp

doi: 10.1111/j.1349-7006.2010.01622.x

Table 1. Clinicopathologic characteristics of lung adenocarcinomas

	PCR	Primary tumor		Brain metastasis
		Multiplex (%)	Nested (%)	Both (%)
No. of cases	–	275	138	22
Gender	Male	161 (59)	81 (59)	15 (68)
	Female	114 (41)	57 (41)	7 (32)
Age (years)	Mean	60.7	62.0	57.3
	Range	30–84	30–84	48–74
Pathological stage	I	201 (73)	124 (90)	–
	II	27 (10)	6 (4)	–
	III	45 (16)	8 (6)	–
	IV	2 (1)	0 (0)	–
Smoking history	Smoker	71 (55)	69 (58)	15 (68)
	Nonsmoker	57 (45)	51 (43)	7 (32)
	Unknown	147	18	0
p53 mutation	+	34 (32)	34 (33)	16 (73)
	–	72 (68)	70 (67)	6 (27)
	ND	169	34	0

ND, not determined.

PCR buffer, 2.5 mM $MgCl_2$, 0.2 mM dNTPs, 0.025 U Taq polymerase, 3 nM primers, and 10 ng template DNA. Amplifications were performed with the following cycling profiling using a GeneAmp PCR system 9700 apparatus (Applied Biosystems, Foster City, CA, USA): Taq polymerase activation by incubation at 95°C for 1 min, followed by 40 cycles of denaturation at 94°C for 30 s, annealing at 70°C for 90 s, and elongation at 72°C for 60 s. Five micro liters of the amplicons were analyzed by electrophoresis on 3% agarose gels and ethidium bromide staining.

Nested PCR with HPV type-specific primers. Sequences from the upstream regulatory region (URR) to the E7 region of HPV 16 and HPV 18 were first amplified by PCR with outer primers, and the HPV 16 E6/E7 and HPV 18 E6 regions were secondly amplified by nested PCR with inner primers, as reported previously.[20] The primer sequences are shown in Supplementary Table S2. The first round of PCR was performed under the following conditions: Taq polymerase activation at 95°C for 1 min, followed by 35 cycles of denaturation at 95°C for 1 min, annealing at 60°C for 1 min, and elongation at 72°C for 1 min. The second round of PCR was performed as follows: 95°C for 1 min, followed by 20 cycles of denaturation for 1 min at 95°C, 1 min of annealing at 60°C, and 1 min of elongation at 72°C. Polymerase chain reaction (PCR) was performed with a Takara Taq with a volume of 20 μL containing 1× PCR buffer, 0.2 mM dNTPs, 0.05 U Taq polymerase, 2 nM of primers, and 10 ng of template DNA for the first round PCR and 1 μL of the first round PCR products for the second round PCR using a GeneAmp PCR system 9700 apparatus (Applied Biosystems).

Mutation analysis of the *p53* gene. A total of 106 of the 275 primary lung AdCs and all of the 22 metastatic lung AdCs were previously examined for mutations in exons 4–8 of the *p53* gene by genomic PCR and direct sequencing.[21,22] All of the 91 lung cancer cell lines were examined for mutations in exons 2–11 covering all the coding sequences of the p53 gene by genomic PCR and direct sequencing as previously described.[18,23] Sequence data for the cell lines obtained in this study were compared with those of the Catalogue of Somatic Mutations in Cancer (COSMIC) (http://www.sanger.ac.uk/cosmic/).[24]

Results

Detection of HPV 16, 18, and 33 DNA by multiplex PCR. Recently, Nishiwaki *et al.* developed a rapid and sensitive multiplex PCR-based HPV genotyping method that allows the simultaneous amplification of 16 different HPV genotypes in a single tube reaction.[19] This method is based on the amplification of multiple HPV-DNA sequences with a set of HPV type-specific primers, and the HPV types are visually distinguished by the size of amplified fragments after separation by gel electrophoresis. Since DNA for HPV 16, 18, and 33 types has been frequently detected in lung AdC cells in East Asia, four primer sets for these three HPV types, in addition to a primer set for a control genome sequence, were used in this study. Two sets of primers were prepared for the amplification of the HPV 16 DNA[19] because of a possible high prevalence of HPV 16 DNA integration in lung AdC genomes.

The sensitivity and specificity of this method was validated using genomic DNA from three cervical cancer cell lines, CaSki, SiHa, and HeLa, and a lung cancer cell line, A549. Human papillomavirus (HPV) 16 has been shown to be integrated into chromosomal DNA in the CaSki and SiHa cell lines, while HPV 18 is integrated in the HeLa cell line.[25–27] A cell line with integration of HPV 33 was not available; therefore, HPV 33 containing plasmid DNA was mixed with A549 cell DNA as a ratio of one copy of HPV 33 DNA per diploid human genome. Specific DNA fragments for HPV 16, 18, and 33 of different sizes from each other were successfully amplified with the control genomic DNA fragment (Genome in Fig. 1) in CaSki, SiHa, and HeLa cells, as well as A549 cells mixed with HPV 33 DNA (Fig. 1). Two bands for HPV 16 DNA (HPV16-U and HPV16-L) were detected in CaSKi and SiHa cell DNA, while a band for HPV 18 DNA was detected in HeLa cell DNA. Human papillomavirus (HPV) 33-specific DNA was amplified from the mixture of plasmid DNA and A549 cell DNA, while no HPV-specific DNA was amplified from A549 cell DNA. Therefore, by this method, three different HPV types were successfully identified and distinguished by the difference in the sizes of amplified DNA. To determine the sensitivity of this method, each sample was serially diluted and mixed with A549 cell DNA to obtain genomic DNA with 0.1–1.0 copies of each HPV-DNA. Approximately 600 copies of HPV 16 DNA are integrated in CaSki cells, one to two copies of HPV 16 DNA are integrated in SiHa cells, and 20–50 copies of HPV 18 DNA are integrated in HeLa cells.[25–27] As shown in Figure 1, 0.1–1.0 copies of the HPV-DNA sequence per cell were detected by this method. Therefore, this method allowed us to detect one copy of HPV 16, 18, and/or 33 DNA integrated in chromosomal DNA of human cells. Further validation of this method was performed using DNA isolated from 18 primary cervical cancers because the presence of the HPV 16/18 DNA in these tumors was previously determined by Southern blot analysis.[28,29] Human papillomavirus (HPV) types detected by multiplex PCR analysis were completely the same as those by Southern blot analysis, and the sensitivity of multiplex PCR analysis for detection of HPV 16 DNA was higher than that of Southern blot analysis. Four cases negative for HPV 16 DNA by Southern blot analysis were positive by multiplex PCR analysis (data not shown). Therefore, we concluded that the sensitivity of the multiplex PCR analysis is higher than that of Southern blot analysis for detection of HPV 16 DNA in cancer cells.

We then applied this method for detection of HPV 16/18/33 DNA in 275 primary lung AdCs and 22 metastatic lung AdCs to the brain (Table 1). However, HPV-specific DNA was not amplified in any of these 297 lung AdCs. Thus, it was strongly suggested that HPV 16/18/33 DNA is not integrated in the chromosomal DNA of these lung AdCs.

Detection of HPV 16 and 18 DNA by nested PCR. It was reported that only a part of HPV-DNA, from the URR to the E6/E7 region, is commonly integrated in chromosomal DNA of cervical cancer cells, and that deletions of other regions occur in the course of viral DNA integration into host cell DNA.[25,26,30]

doi: 10.1111/j.1349-7006.2010.01622.x

Table 2. Status of the *p53* gene in 91 lung cancer cell lines

No.	Cell line	Hist.	Amino acid	Nucleotide
Point mutation				
1	ABC1	AdC	p.P278S	c.832C>T
2	CALU-3	AdC	p.M237I	c.711G>T
3	HCC44	AdC	p.S94X+ p.R175L	c.281C>G+ c.524G>T
4	HCC78	AdC	p.S241F	c.722C>T
5	HCC193	AdC	p.R248Q	c.743G>A
6	HCC515	AdC	p.L194F	c.580C>T
7	Ma10	AdC	p.G245V	c.734G>T
8	Ma17	AdC	p.Y126C	c.377A>G
9	Ma24	AdC	p.R337C	c.1009C>T
10	H23	AdC	p.M246I	c.738G>C
11	H441	AdC	p.R158L	c.473G>T
12	H820	AdC	p.T284P	c.850A>C
13	H1437	AdC	p.R267P	c.800G>C
14	H1975	AdC	p.R273H	c.818G>A
15	H2009	AdC	p.R273L	c.818G>T
16	H2087	AdC	p.V157F	c.469G>T
17	H2122	AdC	p.Q16L+ p.C176F	c.527G>T+ c.47A>T
18	H2126	AdC	p.E62X	c.184G>T
19	PC3	AdC	p.R282W	c.844C>T
20	PC7	AdC	p.H214R	c.641A>G
21	PC9	AdC	p.R248Q	c.743G>A
22	PC14	AdC	p.R248W	c.742C>T
23	RERF-LCMS	AdC	p.R248L	c.743G>T
24	RERF-LC-OK	AdC	p.F113C	c.338T>G
25	VMRC-LCD	AdC	p.R175H	c.524G>A
26	II-18	AdC	p.K164X	c.490A>T
27	H322	AdC	p.R248L	c.743G>T
28	EBC1	SqC	p.E171X	c.511G>T
29	LC1/Sq	SqC	p.M237I	c.711G>T
30	LK2	SqC	p.V272M	c.814G>A
31	HCC15	SqC	p.D259V	c.776A>T
32	H520	SqC	p.W146X	c.438G>A
33	SK-MES-1	SqC	p.E298X	c.892G>T
34	PC10	SqC	p.G245C	c.733G>T
35	HCC366	ASC	p.Y220C	c.659A>G
36	H596	ASC	p.G245C	c.733G>T
37	Lu65	LCC	p.E11Q	c.31G>C
38	Ma2	LCC	p.R175H	c.524G>A
39	Ma25	LCC	p.M237I	c.711G>T
40	H661	LCC	p.R158L+ p.S215I	c.473G>T+ c.644G>T
41	H1155	LCC	p.R273H	c.818G>A
42	PC13	LCC	p.G334V	c.1001G>T
43	HCC33	SCLC	p.C242Y	c.725G>A
44	Lu134	SCLC	p.P278L	c.833C>T
45	Lu135	SCLC	p.G244C	c.730G>T
46	Lu139	SCLC	p.V157F	c.469G>T
47	N417	SCLC	p.E298X	c.892G>T
48	H69	SCLC	p.E171X	c.511G>T
49	H128	SCLC	p.E62X	c.184G>T
50	H345	SCLC	p.Y236C	c.707A>G
51	H446	SCLC	p.Q154V	c.461G>T
52	H841	SCLC	p.C242S	c.724A>T
53	H1184	SCLC	p.G334V	c.1001G>T
54	H1450	SCLC	p.L194R	c.581T>G
55	H1607	SCLC	p.P151H	c.452C>A
56	H1963	SCLC	p.V147D+ p.H214R	c.440T>A+ c.641A>G
57	H2107	SCLC	p.K101X	c.301A>T
58	H2141	SCLC	p.R209X	c.625A>T
59	H2171	SCLC	p.Q144X	c.430C>T
60	H2195	SCLC	p.V157F	c.469G>T
61	H1618	SCLC	p.R248L	c.743G>T
62	H187	SCLC	p.S241C	c.722C>G
63	H510	SCLC	p.R282G	c. 844C>G
64	H1770	Neuroendocrine	p.R248W	c.741-742CC>TT
Small insertion/deletion (≤9 nucleotides)				
1	Ma29	AdC	p.V121fs	c.363delT
2	H522	AdC	p.P191fs	c.572delC
3	H1648	AdC	p.L35fs	c.103-104insT
4	HCC95	SqC	p.G334fs	c.1000(-1003) 1G del
5	H157	SqC	p.L35fs+ p.E298X	c.103-104insT+ c.892G>T
6	H727	Carcinoid	p.Q165-S166 insYKQ	c.496-497ins9
Large deletion				
1	H358	AdC	p?	Large deletion
2	H1299	LCC	p?	Large deletion
Splicing-site mutation				
1	H1703	AdC	p.G262fs	g. Ivs8 +1g>t
2	H1819	AdC	p.A307fs	g. Ivs9 +1g>t
3	H2347	AdC	p.Y126fs	g.375G>A
4	H1650	AdC	p.V225fs	g.Ivs6 -2a>g
5	Sq1	SqC	p.Y126fs	g. Ivs4 +2t>c
6	H82	SCLC	p.Y126fs	g.375G>T
7	H209	SCLC	p.V225fs	g. Ivs6 -2a>t
8	H526	SCLC	p.S33fs	g. Ivs3 -1g>c
9	H1339	SCLC	p.I332fs	g.Ivs9 +1g>t
Wild type				
1	A427	AdC	—	—
2	A549	AdC	—	—
3	Ma12	AdC	—	—
4	Ma26	AdC	—	—
5	H1395	AdC	—	—
6	H226	SqC	—	—
7	Lu99A	LCC	—	—
8	H460	LCC	—	—
9	Lu24	SCLC	—	—
10	Ms18	SCLC	—	—

p, c, and g indicate protein, cDNA, and genomic DNA.
AdC, adenocarcinoma; ASC, adenosquamous carcinoma; LCC, large-cell carcinoma;
SCLC, small-cell lung carcinoma; SqC, squamous cell carcinoma.

The primers for HPV 16, 18, and 33 in the above multiplex PCR analysis were designed to amplify the E1 or L2 region (Supplementary Table S2).[19] Therefore, it was possible that multiplex PCR analysis failed to detect the HPV-DNA sequences because of integration of truncated HPV genomes without the E1 and L2 regions into host cell DNA. To pursue the possible integration of HPV 16 and 18 DNA in lung AdC cells, we performed a nested PCR analysis for the E6 and E7 regions of HPV 16 and 18. The URR to the E7 region of both HPV 16 and 18 genomes was first amplified using outer primers, then, the E6 to E7 region of the HPV 16 DNA and the E6 region of the HPV 18 DNA were amplified using inner primers (Supplementary Table S2), respectively, according to the method previously described.[20] As in the multiplex PCR analysis, HPV 16- and 18-specific DNA fragments were successfully amplified from the CaSki, SiHa, and HeLa cell lines, but not from A549. Next, 138 of the 275 primary AdCs and all of the 22 metastatic AdCs used for

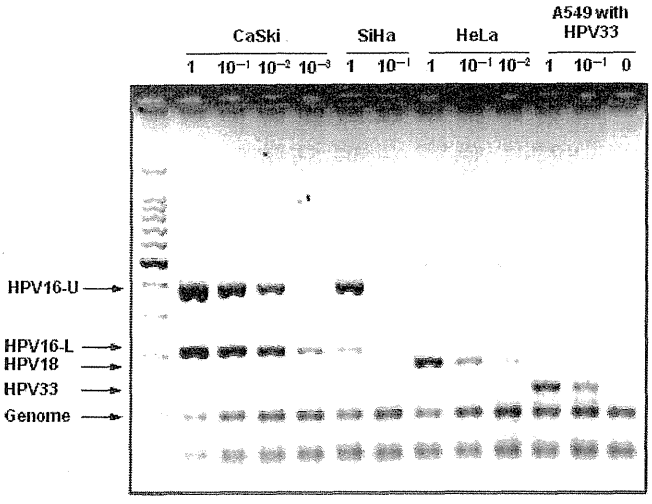

Fig. 1. Detection of human papillomavirus (HPV) 16, 18, and 33 DNA in cervical cancer cell lines by multiplex PCR analysis. Specificity and sensitivity for detection of HPV 16, 18, and 33 DNA. Polymerase chain reaction (PCR) was performed using DNA from CaSki (~600 copies of HPV 16 integrated), SiHa (1–2 copies of HPV 16 integrated), HeLa (20–50 copies of HPV 18 integrated), and A549 cells with/without HPV 33 containing plasmid DNA. Each sample was serially diluted with A549 cell DNA up to the copy number of 0.1–1.0 per cell for HPV-DNA. Five micro liters of the amplicons were analyzed by electrophoresis on 3% agarose gels and ethidium bromide staining. 100 bp DNA Ladder (Takara, Shiga, Japan) was used as a size marker.

multiplex PCR analysis were subjected to nested PCR analysis (Table 1). However, none of them showed positive signals for the E6/E7 regions of the HPV 16 or 18. The results of multiplex PCR analysis as well as those of nested PCR analysis strongly indicated that HPV 16 and 18 are not integrated in lung AdCs developed in Japan, at least in the Tokyo area.

Absence of HPV 16, 18, and 33 DNA sequences in lung cancer cell lines. We next attempted to detect HPV 16, 18, and 33 DNA in a panel of 91 human lung cancer cell lines established in either Japan or the USA. Among the 91 cell lines, 30 originated from Japanese, 42 from Caucasians, and five from African-Americans. Detailed information was not available for the remaining 14 cell lines. Forty cell lines were derived from AdC and the remaining 51 were from other histological types. Both multiplex PCR and nested PCR were performed on all of these cell lines. However, no HPV-specific signals were obtained in any of these cell lines. Therefore, HPV 16, 18, and 33 DNA is not integrated in the 91 lung cancer cell lines established in Japan and the USA. Eleven cell lines were derived from SqC, and 27 cell lines were derived from SCLC; therefore, HPV 16/18/33 integration was not evident in any major histological types of lung cancer.

Status of p53 mutations in lung cancer cell lines. We previously examined for p53 mutations in 106 of the 275 primary tumors and all 22 brain metastases,[21,22] and the mutations were detected in 34 of the 106 primary tumors (32%) and 16 of the 22 brain metastases (73%) (Table 1). We recently reported the status of p53 mutations in 87 of the 91 cell lines analyzed in the present study.[18] In that study, mutation data of several cell lines were obtained not only by direct sequencing of the p53 coding regions but also from the COSMIC database, and the mutations were detected in 70 of the 87 cell lines (80%). However, during this study, we noticed that data for p53 mutations are not the same among three major databases, COSMIC, UMD_TP53 database (http://p53.free.fr), and IARC p53 database (http://www-p53.iarc.fr).[24,31,32] Absence of HPV 16/18/33 integration as well as p53 mutations in 17 lung cancer cell lines prompted us to re-investigate the status of p53 mutations in these cell lines. Therefore, the p53 mutation status in all the 91 cell lines was determined by direct sequencing of all the coding exons, from exon 2 to exon 11, together with exon–intron boundaries of these exons (Table 2). If mutations were detected in the exon–intron boundaries, a possible occurrence of splicing abnormalities due to the mutations was examined by direct sequencing of p53 cDNA products from the corresponding cell lines. Point mutations were detected in 64 of the 91 cell lines, small insertions/deletions in six of them, and large deletions in two of them. Splice-site mutations were detected in nine cell lines, in which shifts of open reading frames due to either exon skipping or intron retention were confirmed. Accordingly, only 10 cell lines were shown to carry the wild-type *p53* gene and express normal p53 protein, including five of the 40 AdC cell lines.

The status of 36 cell lines was not available in COSMIC and thus was defined by our studies (Supplementary Table S3-1) ([18,21–23], this study). The status of 45 cell lines was concordant between our data and COSMIC data (Supplementary Table S3-2), whereas that of the remaining 10 cell lines was discordant (Supplementary Table S3-3). Therefore, although 10 of the 91 lung cancer cell lines carry the wild-type *p53* gene, HPV 16, 18, or 33 are not integrated in these cell lines.

Discussion

To detect HPV-DNA in lung cancer cells, we applied two different PCR methods with HPV type-specific primers, one-step multiplex PCR[19] and nested PCR,[20] because PCR with type-specific primers was reported to be more sensitive than PCR with consensus primers to detect HPV-DNA sequences in human cell DNA.[7] The prevalence and genotype distribution of HPV in cervical cancer precursor lesions defined by one-step multiplex PCR was reported to be compatible with several previous data.[19] In addition, by using these methods, HPV 16 and 18 DNA was distinguishably and efficiently amplified from three cervical cancer cell lines. Therefore, the lack of HPV 16, 18, and 33 DNA in primary lung AdC as well as in lung cancer cell lines would not be due to the low sensitivity of this method for HPV detection. Accordingly, it was concluded from this study that HPV 16, 18, and 33 are not (or are rarely) integrated in lung AdC genomes in the Japanese, particularly those living in the Tokyo area. Lung cancer cell lines analyzed in this study have been established in either Japan or the USA, and consist of all major histological types of lung cancer. Absence of HPV 16/18/33 infection in primary lung AdCs in the US population and lung cancer cell lines established in the USA was previously reported.[33–35] Therefore, the results in the cell lines are consistent with the results in primary AdCs in both Japan and the USA. Indeed, we further attempted to detect HPV-associated DNA sequences in these cell lines by PCR under several low stringent conditions using a set of consensus primers for HPV 16, 18, and 33. However, no HPV-specific signals were detected in any of the 91 lung cancer cell lines examined (data not shown). Therefore, we concluded that no HPV 16/18/33 DNA is integrated in these cell lines. Accordingly, HPV infection seems not to play an important role in the development of lung cancer in Japan nor in the USA, although it is still possible that other HPV types play some role in its development.

A Taiwanese study reported that female never-smokers with lung cancer who were older than 60 years of age had a significantly higher prevalence of HPV 16/18 infections.[8] However, in Korean lung cancer patients, HPV 16/18/33 infections were not associated with gender, smoking status, and histological type.[10] In a study in China, HPV 16/18 infections were not correlated with any clinicopathological parameter, including

doi: 10.1111/j.1349-7006.2010.01622.x

age, gender, smoking status, and histological type, either.[9] In this study, 41% (121/297) and 43% (64/150) of AdC patients were female and non-smokers, respectively (Table 1). Therefore, the etiological role of HPV 16/18 in lung carcinogenesis in non-smokers seems to be restricted to certain geographic areas, and in Japan, HPV 16/18 infection does not play a causative role in the development of lung AdC in female non-smokers.

An inverse correlation of HPV 16/18 E6 protein expression with p53 expression was also reported in Taiwanese lung tumors.[36] However, in a study in China, there was a relationship between the presence of HPV 16/18 DNA and abnormal p53 protein accumulation.[37] Therefore, association of HPV infection with p53 inactivation is still unclear in lung cancer. We previously examined for p53 mutations in 128 of 297 lung AdCs analyzed in this study, and the mutations were detected in 50 cases (39%) (Table 1); therefore, it was possible that HPV is infected in another 78 cases. However, none of the 78 lung AdCs carried HPV 16/18/33 DNA in their genomes. Accordingly, HPV 16/18/33 infections appear to play a limited role in the development of lung AdC in Japan. These results prompted us to analyze comprehensively the status of the *p53* gene in a large panel of lung cancer cell lines. The *p53* gene is inactivated not only by mutations in the coding regions, but also by splicing abnormalities caused by mutations in the exon–intron boundaries and homozygous deletions, and the incidence of p53 genetic alterations in total was 89% (81/91). Therefore, although 10 of the 91 cell lines were shown to carry the wild-type *p53* gene, no HPV 16/18/33 DNA was detected in these cell lines. Since the status of the *p53* gene in these cell lines was not consistent among several databases and reports, the results provided here will be highly informative to diverse scientists using these cell lines for molecular and biological studies.

In Japan, HPV-DNA has been detected in <10% of lung AdC in Chiba and Hokkaido, and ~20% in Okinawa (Supplementary Table S1). Therefore, we cannot totally rule out the involvement of HPV infection in the etiology of lung AdC in Japan. However, the present results strongly indicate that HPV infection plays only a limited role, if any, in the development of lung AdC in Japan.

Acknowledgments

This work was supported by Grants-in-Aid from the Ministry of Health, Labor and Welfare for the 3rd-Term Comprehensive 10-year Strategy for Cancer Control and for Cancer Research (16-1) and a Grant-in-Aid for the Program for Promotion of Fundamental Studies in Health Sciences of the National Institute of Biomedical Innovation (NiBio). We are grateful to Drs R. Nishikawa and K. Mishima of the Saitama Medical University Hospital for preparation of metastatic lung adenocarcinoma specimens.

Disclosure Statement

The authors have no conflict of interest.

References

1 zur Hausen H. Papillomaviruses in the causation of human cancers - a brief historical account. *Virology* 2009; **384**: 260–5.
2 Werness BA, Levine AJ, Howley PM. Association of human papillomavirus types 16 and 18 E6 proteins with p53. *Science* 1990; **248**: 76–9.
3 Scheffner M, Werness BA, Huibregtse JM, Levine AJ, Howley PM. The E6 oncoprotein encoded by human papillomavirus types 16 and 18 promotes the degradation of p53. *Cell* 1990; **63**: 1129–36.
4 Nakanishi H, Matsumoto S, Iwakawa R *et al.* Whole genome comparison of allelic imbalance between noninvasive and invasive small-sized lung adenocarcinomas. *Cancer Res* 2009; **69**: 1615–23.
5 Sun S, Schiller JH, Gazdar AF. Lung cancer in never smokers–a different disease. *Nat Rev Cancer* 2007; **7**: 778–90.
6 Klein F, Kotb WF, Petersen I. Incidence of human papilloma virus in lung cancer. *Lung Cancer* 2009; **65**: 13–8.
7 Srinivasan M, Taioli E, Ragin CC. Human papillomavirus type 16 and 18 in primary lung cancers–a meta-analysis. *Carcinogenesis* 2009; **30**: 1722–8.
8 Cheng YW, Chiou HL, Sheu GT *et al.* The association of human papillomavirus 16/18 infection with lung cancer among nonsmoking Taiwanese women. *Cancer Res* 2001; **61**: 2799–803.
9 Fei Y, Yang J, Hsieh WC *et al.* Different human papillomavirus 16/18 infection in Chinese non-small cell lung cancer patients living in Wuhan, China. *Jpn J Clin Oncol* 2006; **36**: 274–9.
10 Park MS, Chang YS, Shin JH *et al.* The prevalence of human papillomavirus infection in Korean non-small cell lung cancer patients. *Yonsei Med J* 2007; **48**: 69–77.
11 Hirayasu T, Iwamasa T, Kamada Y, Koyanagi Y, Usuda H, Genka K. Human papillomavirus DNA in squamous cell carcinoma of the lung. *J Clin Pathol* 1996; **49**: 810–7.
12 Miyagi J, Kinjo T, Tsuhako K *et al.* Extremely high Langerhans cell infiltration contributes to the favourable prognosis of HPV-infected squamous cell carcinoma and adenocarcinoma of the lung. *Histopathology* 2001; **38**: 355–67.
13 Kinoshita I, Dosaka-Akita H, Shindoh M *et al.* Human papillomavirus type 18 DNA and E6-E7 mRNA are detected in squamous cell carcinoma and adenocarcinoma of the lung. *Br J Cancer* 1995; **71**: 344–9.
14 Hiroshima K, Toyozaki T, Iyoda A *et al.* Ultrastructural study of intranuclear inclusion bodies of pulmonary adenocarcinoma. *Ultrastruct Pathol* 1999; **23**: 383–9.
15 Sobin LH, Wittekind CH, eds. *TNM classification of malignant tumours*, 6th ed. New York: Wiley-Liss; 2002: p. 99–103.
16 Sakamoto H, Mori M, Taira M *et al.* Transforming gene from human stomach cancers and a noncancerous portion of stomach mucosa. *Proc Natl Acad Sci U S A* 1986; **83**: 3997–4001.
17 Kohno T, Otsuka A, Girard L *et al.* A catalog of genes homozygously deleted in human lung cancer and the candidacy of PTPRD as a tumor suppressor gene. *Genes Chromosomes Cancer* 2010; **49**: 342–52.
18 Blanco R, Iwakawa R, Tang M *et al.* A gene-alteration profile of human lung cancer cell lines. *Hum Mutat* 2009; **30**: 1199–206.
19 Nishiwaki M, Yamamoto T, Tone S *et al.* Genotyping of Human Papillomaviruses by a Novel One-Step Typing Method with Multiplex PCR and Clinical Applications. *J Clin Microbiol* 2008; **46**: 1161–8.
20 Wu EQ, Zhang GN, Yu XH *et al.* Evaluation of high-risk human papillomaviruses type distribution in cervical cancer in Sichuan province of China. *BMC Cancer* 2008; **8**: 202.
21 Tomizawa Y, Kohno T, Fujita T *et al.* Correlation between the status of the p53 gene and survival in patients with stage I non-small cell lung carcinoma. *Oncogene* 1999; **18**: 1007–14.
22 Iwakawa R, Kohno T, Anami Y *et al.* Association of p16 homozygous deletions with clinicopathological characteristics and EGFR/KRAS/p53 mutations in lung adenocarcinoma. *Clin Cancer Res* 2008; **14**: 3746–53.
23 Matsumoto S, Iwakawa R, Takahashi K *et al.* Prevalence and specificity of LKB1 genetic alterations in lung cancers. *Oncogene* 2007; **26**: 5911–8.
24 Forbes SA, Tang G, Bindal N *et al.* COSMIC (the Catalogue of Somatic Mutations in Cancer): a resource to investigate acquired mutations in human cancer. *Nucleic Acids Res* 2010; **38**(Database issue): D652–7.
25 Schwarz E, Freese UK, Gissmann L *et al.* Structure and transcription of human papillomavirus sequences in cervical carcinoma cells. *Nature* 1985; **314**: 111–4.
26 Baker CC, Phelps WC, Lindgren V, Braun MJ, Gonda MA, Howley PM. Structural and transcriptional analysis of human papillomavirus type 16 sequences in cervical carcinoma cell lines. *J Virol* 1987; **61**: 962–71.
27 Yee C, Krishnan-Hewlett I, Baker CC, Schlegel R, Howley PM. Presence and expression of human papillomavirus sequences in human cervical carcinoma cell lines. *Am J Pathol* 1985; **119**: 361–6.
28 Yokota J, Tsukada Y, Nakajima T *et al.* Loss of heterozygosity on the short arm of chromosome 3 in carcinoma of the uterine cervix. *Cancer Res* 1989; **49**: 3598–601.
29 Kohno T, Takayama H, Hamaguchi M *et al.* Deletion mapping of chromosome 3p in human uterine cervical cancer. *Oncogene* 1993; **8**: 1825–32.
30 Pett M, Coleman N. Integration of high-risk human papillomavirus: a key event in cervical carcinogenesis? *J Pathol* 2007; **212**: 356–67.
31 Berglind H, Pawitan Y, Kato S, Ishioka C, Soussi T. Analysis of p53 mutation status in human cancer cell lines: a paradigm for cell line cross-contamination. *Cancer Biol Ther* 2008; **7**: 699–708.
32 Petitjean A, Mathe E, Kato S *et al.* Impact of mutant p53 functional properties on TP53 mutation patterns and tumor phenotype: lessons from recent developments in the IARC TP53 database. *Hum Mutat* 2007; **28**: 622–9.

33 Yousem SA, Ohori NP, Sonmez-Alpan E. Occurrence of human papillomavirus DNA in primary lung neoplasms. *Cancer* 1992; **69**: 693–7.
34 Wistuba II, Behrens C, Milchgrub S *et al.* Comparison of molecular changes in lung cancers in HIV-positive and HIV-indeterminate subjects. *JAMA* 1998; **279**: 1554–9.
35 Shimizu E, Coxon A, Otterson GA *et al.* RB protein status and clinical correlation from 171 cell lines representing lung cancer, extrapulmonary small cell carcinoma, and mesothelioma. *Oncogene* 1994; **9**: 2441–8.
36 Cheng YW, Wu MF, Wang J *et al.* Human papillomavirus 16/18 E6 oncoprotein is expressed in lung cancer and related with p53 inactivation. *Cancer Res* 2007; **67**: 10686–93.
37 Wang Y, Wang A, Jiang R *et al.* Human papillomavirus type 16 and 18 infection is associated with lung cancer patients from the central part of China. *Oncol Rep* 2008; **2**: 333–9.

Supporting Information

Additional Supporting Information may be found in the online version of this article:

Table S1. Prevalence of human papillomavirus (HPV) 16, 18, and 33 in lung adenocarcinomas in East Asia.

Table S2. Primer sequences for detection of human papillomavirus (HPV) DNA in cancer cell DNA.

Table S3-1. p53 status defined in our studies but not registered in the COSMIC database.

Table S3-2. Concordance of p53 status defined in our studies and registered in the COSMIC database.

Table S3-3. Discordance of p53 status defined in our studies and registered in the COSMIC database.

Please note: Wiley-Blackwell are not responsible for the content or functionality of any supporting materials supplied by the authors. Any queries (other than missing material) should be directed to the corresponding author for the article.

doi: 10.1111/j.1349-7006.2010.01622.x

The EMBO Journal (2010) 29, 2802–2812 | © 2010 European Molecular Biology Organization | All Rights Reserved 0261-4189/10
www.embojournal.org

THE EMBO JOURNAL

14-3-3γ mediates Cdc25A proteolysis to block premature mitotic entry after DNA damage

Kousuke Kasahara[1], Hidemasa Goto[1,2], Masato Enomoto[1,2], Yasuko Tomono[3], Tohru Kiyono[4] and Masaki Inagaki[1,2,*]

[1]Division of Biochemistry, Aichi Cancer Center Research Institute, Nagoya, Aichi, Japan, [2]Department of Cellular Oncology, Nagoya University Graduate School of Medicine, Nagoya, Aichi, Japan, [3]Division of Molecular and Cell Biology, Shigei Medical Research Institute, Okayama, Okayama, Japan and [4]Virology Division, National Cancer Center Research Institute, Chuo-ku, Tokyo, Japan

14-3-3 proteins control various cellular processes, including cell cycle progression and DNA damage checkpoint. At the DNA damage checkpoint, some subtypes of 14-3-3 (β and ζ isoforms in mammalian cells and Rad24 in fission yeast) bind to Ser345-phosphorylated Chk1 and promote its nuclear retention. Here, we report that 14-3-3γ forms a complex with Chk1 phosphorylated at Ser296, but not at ATR sites (Ser317 and Ser345). Ser296 phosphorylation is catalysed by Chk1 itself after Chk1 phosphorylation by ATR, and then ATR sites are rapidly dephosphorylated on Ser296-phosphorylated Chk1. Although Ser345 phosphorylation is observed at nuclear DNA damage foci, it occurs more diffusely in the nucleus. The replacement of endogenous Chk1 with Chk1 mutated at Ser296 to Ala induces premature mitotic entry after ultraviolet irradiation, suggesting the importance of Ser296 phosphorylation in the DNA damage response. Although Ser296 phosphorylation induces the only marginal change in Chk1 catalytic activity, 14-3-3γ mediates the interaction between Chk1 and Cdc25A. This ternary complex formation has an essential function in Cdc25A phosphorylation and degradation to block premature mitotic entry after DNA damage.

The EMBO Journal (2010) **29**, 2802–2812. doi:10.1038/emboj.2010.157; Published online 16 July 2010
Subject Categories: cell cycle; genome stability & dynamics
Keywords: Cdc25; Chk1; DNA damage checkpoint; phosphorylation; 14-3-3

Introduction

The cell cycle checkpoint is a fundamental mechanism, not only for monitoring genomic stability, but also for coordinating repair and cell cycle progression. The protein kinase cascade from ATR to Chk1 has important functions in the DNA damage checkpoint (Zhou and Elledge, 2000; Bartek and Lukas, 2003; Kastan and Bartek, 2004). In response to damaged DNA or stalled replication, ATR phosphorylates Chk1 at Ser317 and Ser345; this phosphorylation is considered to elevate the catalytic activity of Chk1 (Zhao and Piwnica-Worms, 2001; Walker *et al*, 2009). Chk1 then phosphorylates and inhibits Cdc25 family phosphatases, which consist of Cdc25A, B and C in human cells (Boutros *et al*, 2007). For example, Chk1 induces Cdc25A-Ser76 phosphorylation, which results in βTrCP-dependent Cdc25A degradation (Busino *et al*, 2003, 2004; Jin *et al*, 2003; Neely and Piwnica-Worms, 2003; Melixetian *et al*, 2009). As Cdc25 dephosphorylates cyclin-dependent kinases (Cdks) at an inhibitory phosphorylation site (Cdk1 at Tyr15), Cdc25 inhibition results in Cdk inactivation and cell cycle arrest (Jackman and Pines, 1997; Zhou and Elledge, 2000; Bartek and Lukas, 2003; Kastan and Bartek, 2004).

The DNA damage checkpoint response is also modulated by phosphoserine/phosphothreonine-binding proteins/domains, such as 14-3-3 proteins, FHA domains and BRCT domains (Mohammad and Yaffe, 2009). Studies in fission yeast first suggested that there was a correlation between 14-3-3 proteins and checkpoint control: Rad24, one of 14-3-3 proteins in fission yeast, was identified in a search for irradiation-sensitive mutants (Ford *et al*, 1994). Further studies indicated that Chk1 and 14-3-3 proteins act through Cdc25 (Pines, 1999). In both human cells and fission yeast, Chk1 phosphorylates Cdc25 on a conserved serine residue (human Cdc25C on Ser216), creating a phosphoserine-binding site for 14-3-3 (Furnari *et al*, 1997; Peng *et al*, 1997; Sanchez *et al*, 1997). As Ser216 on human Cdc25C appears to be highly phosphorylated by C-TAK1 in the absence of DNA damage (Peng *et al*, 1998; Russell, 1998; Zhou and Elledge, 2000), it remains controversial how 14-3-3 modulates the signal from Chk1 to Cdc25 in mammals.

Some subtypes of 14-3-3 (β and ζ isoforms in mammalian cells and Rad24 in fission yeast) also bind Chk1 in a Ser345-phosphorylation-dependent manner (Jiang *et al*, 2003; Dunaway *et al*, 2005). This binding promotes the nuclear retention of Chk1 likely through the masking of NES on Chk1 (Jiang *et al*, 2003; Dunaway *et al*, 2005). As Chk1 is phosphorylated at several sites other than Ser317 and Ser345 (ATR sites) in DNA damage responses (Clarke and Clarke, 2005; Puc *et al*, 2005; Ikegami *et al*, 2008), we postulate that Chk1 phosphorylation at other site(s) may also modulate the checkpoint signalling through 14-3-3 binding. Here, we show that the γ subtype of 14-3-3 also forms a complex with Chk1 when DNA damage occurs. This binding depends on Chk1 autophosphorylation at Ser296, which occurs after ATR-induced phosphorylation of Chk1 (by implication, catalytic activation of Chk1) and then promotes dephosphorylation at the ATR sites. This phosphorylation shift from ATR sites to Ser296 not only has an important function in the spread of Chk1 signals, but also changes the Chk1-binding subtype of 14-3-3 (from β or ζ to γ). The 14-3-3γ serves as a platform between Cdc25A and Ser296-phosphorylated Chk1, promoting Chk1-induced Cdc25A phosphorylation at Ser76, a critical site for its degradation.

*Corresponding author. Division of Biochemistry, Aichi Cancer Center Research Institute, 1-1 Kanokoden, Chikusa-ku, Nagoya, Aichi 464-8681, Japan. Tel: +81 52 762 6111/ext. 7020; Fax: +81 52 763 5233; E-mail: minagaki@aichi-cc.jp

Received: 14 January 2010; accepted: 21 June 2010; published online: 16 July 2010

Results

Ser296 phosphorylation is catalysed by Chk1 itself after phosphorylation by ATR

Chk1 was reported to be phosphorylated not only at Ser317 and Ser345, but also at Ser296 (Clarke and Clarke, 2005) in response to DNA damage, but only limited information has been available about Ser296 phosphorylation. We first produced an antibody that specifically recognizes Chk1 phosphorylated at Ser296 (Figure 1A and B; see also Supplementary Figure S1). Using Chk1 purified from baculovirus-infected Sf9 cells, we performed the *in vitro* autophosphorylation assay. After 30 min of the incubation with [γ-^{32}P] ATP, radioactive phosphates (^{32}P) were incorporated

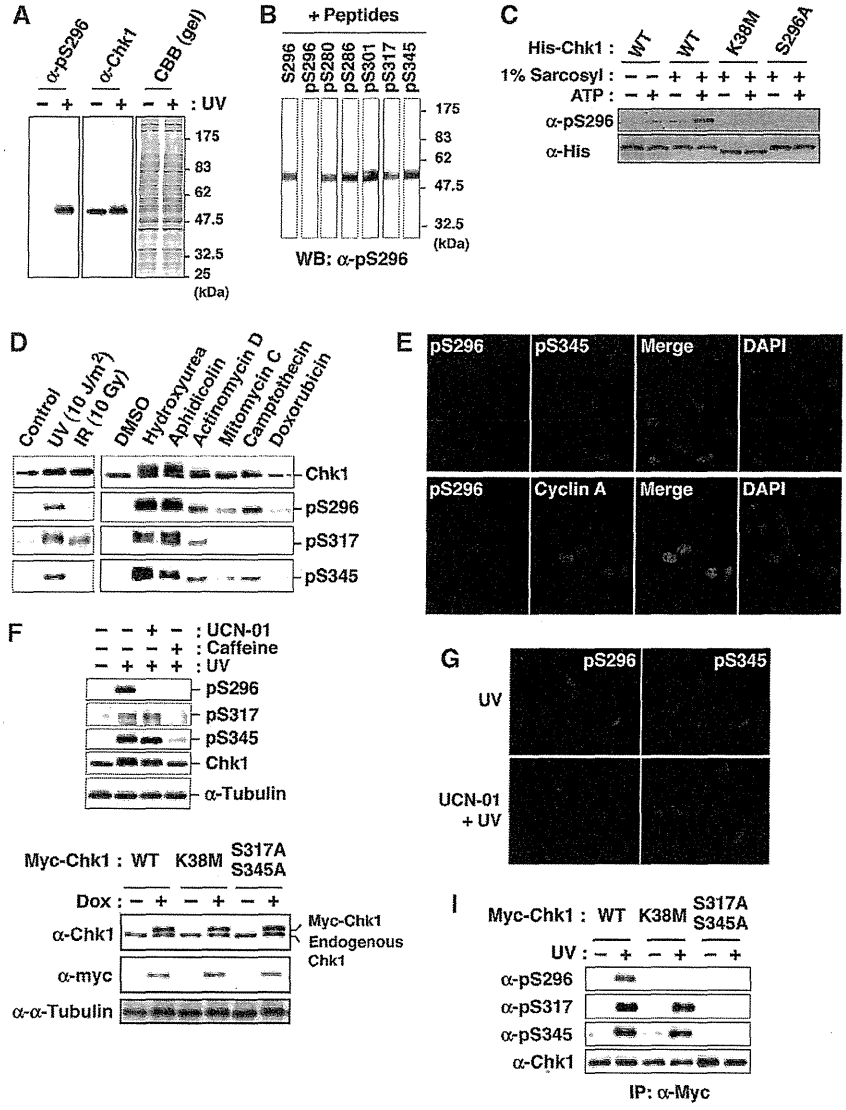

Figure 1 Chk1 autophosphorylation at Ser296. (**A**, **B**) Characterization of an antibody specifically recognizing Chk1 phosphorylation at Ser296. The antibody (α-pS296) reacted specifically with a band corresponding to Chk1 in lysates of UV-irradiated (+) HeLa cells (Ikegami *et al*, 2008), but not of non-treated (−) cells (**A**). Immunoreactivity was impaired specifically by preincubation with pS296 corresponding to Ser296-phosphorylated Chk1, but not with non-phosphorylated peptide S296 and phosphopeptides for other sites within Chk1 (**B**). (**C**) The *in vitro* autophosphorylation assay using 6xHis-ProS2-Chk1 (His-Chk1) expressed in bacteria. *E. coli* strain BL21-CodonPlus®(DE3)-RP was transformed with pCold ProS2 carrying each Chk1. Each 6xHis-ProS2-tagged Chk1 was expressed in the presence of 1 mM IPTG at 15°C for 16 h. *E. coli* cells were lysed in the lysis buffer (40 mM Hepes-NaOH [pH 8.0], 300 mM NaCl, 1% Triton X-100) supplemented with (+) or without (−) 1% sarcosyl. After centrifugation (17 000 *g*) for 10 min at 4°C, the supernatant was rotated with TALON metal affinity resin at 4°C for 1 h. After washing with the lysis buffer and reaction buffer (25 mM Tris–HCl [pH 7.5], 10 mM $MgCl_2$), the beads were incubated in the reaction buffer with (+) or without (−) 10 μM ATP at 30°C for 30 min. Chk1 phosphorylated at Ser296 or total Chk1 was detected through immunoblotting with an anti-pS296 (α-pS296) or anti-His (α-His) antibody, respectively. (**D**) HeLa cells were irradiated with UV, X-rays (IR; 10 Gy) or none (control) and then incubated for an additional 1 h. For treatment with drugs, cells were incubated with 2 mM hydroxyurea, 5 μg/ml aphidicolin, 5 μM actinomycin D, 5 μM mitomycin C, 5 μM camptothecin, 10 μM doxorubicin or 0.1% DMSO (as a solvent control) for 3 h. Extracts were subjected to immunoblotting with the indicated antibodies. (**E**) HeLa cells irradiated with UV were stained with the indicated antibodies and DAPI. (**F**, **G**) Immunoblots (**F**) or immunocytochemistry (**G**) shows effects of pre-treatment with UCN-01 or caffeine on Chk1 phosphorylation in UV-irradiated HeLa cells. (**H**, **I**) Establishment of HeLa cells in which each Myc-Chk1 (WT, K38 M or S317A/S345A) is expressed in a doxycycline (Dox)-dependent manner (**H**). Levels of Chk1 phosphorylation after UV-irradiation (**I**).

into Chk1 wild-type (WT) protein (Supplementary Figure S1E). The electrophoretic mobility of Chk1 was slower after the incubation with ATP; the anti-pS296 on Chk1 (α-pS296) reacted with WT specifically after the incubation (Supplementary Figure S1E). Chk1 mutation at Lys38 to Met (K38M), which lost the catalytic activity, almost completely abolished ^{32}P incorporation, the mobility shift and α-pS296 immunoreactivity (Supplementary Figure S1E). Chk1 mutation at Ser296 to Ala (S296A) reduced ^{32}P incorporation and abolished α-pS296 immunoreactivity. However, S296A did not completely abolish both ^{32}P incorporation and the mobility shift (Supplementary Figure S1E). In the 2D phosphopeptide mapping analysis, S296A induced the disappearance of the radioactive spots 1 and 2, although other major spots (3–6) appeared to remain unchanged on the thin layer plate (Supplementary Figure S1E). To rule out the possibility that a contaminating kinase in insect cells may phosphorylate Chk1-Ser296, we used His-ProS2-Chk1 protein expressed in bacteria (Figure 1C; His-Chk1). In the extraction of protein without sarcosyl, α-pS296 immunoreactivity in WT was observed very weakly even after the incubation with ATP (Figure 1C; 1% sarcosyl: −). On the other hand, the extraction of WT protein with 1% sarcosyl elevated the α-pS296 immunoreactivity after the incubation with ATP much more than without ATP (Figure 1C) (Zhao and Piwnica-Worms, 2001). However, such phenomena were not observed in the case of K38M or S296A (Figure 1C). All these results suggested that Ser296 on Chk1 serves as one of the major autophosphorylation sites *in vitro*.

We next examined Ser296 phosphorylation in the checkpoint response. In response to various DNA damage stimuli and replication disorders, Chk1 phosphorylation at Ser296 was found to occur in a way similar to the phosphorylation at ATR sites (Figure 1D and E). Furthermore, treatment with UCN-01 (a Chk1 kinase inhibitor) attenuated Chk1 phosphorylation at Ser296, but not at ATR sites, although caffeine (an ATR and ATM inhibitor) showed non-specific reduction in phosphorylation rates (Figure 1F and G). Next, we established HeLa cell lines in which Myc-tagged Chk1 was expressed in a tetracycline- or doxycycline (Dox)-dependent manner; the protein level of each exogenous Chk1 was very similar to that of endogenous Chk1 under our experimental conditions (Figure 1H). Although Ser296 phosphorylation in response to ultraviolet (UV) irradiation was observed in WT, it rarely occurred on Chk1 mutated at ATR sites to Ala (S317A/S345A; Figure 1I). In a kinase dead Chk1 mutant (K38M), Ser296 phosphorylation was hardly detected, although Ser317 and Ser345 phosphorylation was observed (Figure 1I). The above observations suggested that Chk1 phosphorylation at Ser296 is catalysed by its own kinase activity, but not by ATR, although it requires pre-phosphorylation at ATR sites, which has implications for the catalytic activation of Chk1 (Zhao and Piwnica-Worms, 2001; Walker *et al*, 2009).

Ser296-phosphorylated Chk1 is rapidly dephosphorylated at ATR sites and distributed throughout the nucleoplasm

We then scrutinized the subcellular distribution of Ser296-phosphorylated Chk1. In UV-irradiated cells, Ser345-phosphorylated Chk1 was observed at nuclear foci of ATR-interacting protein (ATRIP) and the phosphorylated form of RPA32 (an ATR substrate; Figure 2A), in which ATR is considered to be activated (Zou and Elledge, 2003). In contrast, Ser296-phosphorylated Chk1 appeared to distribute diffusely in the nucleus (Figure 2B). In support of this observation, nuclear signals of anti-pS296, but not of anti-pS345, almost completely disappeared after brief extraction with Triton X-100 detergent (Figure 2C). Biochemical fractionation (Figure 2D) also showed that Ser296-phosphorylated Chk1 was clearly detectable in the soluble (S1 plus S2) but not the chromatin (P2) fractions, although Ser317- and Ser345-phosphorylated Chk1 existed in both (Jiang *et al*, 2003; Smits *et al*, 2006). These observations suggest that Ser296-phosphorylated Chk1 is distributed throughout the nucleoplasm, distinct from the localization of Chk1 phosphorylated by ATR.

We further confirmed that only faint signals for anti-pS317/pS345 and -pS296 were apparent in anti-pS296 and -pS345 immunoprecipitates, respectively (Supplementary Figure S2A). These findings raised the new question of why only a few Chk1 molecules are phosphorylated simultaneously at Ser296 and ATR sites despite the fact that Ser296 phosphorylation depends on ATR-induced phosphorylation. One possible explanation is rapid dephosphorylation at ATR sites on Ser296-phosphorylated Chk1. In support of this model, we found that dephosphorylation at ATR sites was remarkably delayed in Chk1 mutated at Ser296 to Ala (S296A), compared with the WT case (Supplementary Figure S2B). In addition, treatment with UCN-01 (Supplementary Figure S2C) or protein phosphatase 2A (PP2A)-specific small-interfering RNA (siRNA) (Supplementary Figure S2D) attenuated the dephosphorylation reaction of ATR sites after the release of hydroxyurea. These observations are consistent with a previous report that PP2A promptly dephosphorylates ATR sites in a Chk1 kinase activity-dependent manner (Leung-Pineda *et al*, 2006). Thus, Ser296 phosphorylation, which occurs only on Chk1 phosphorylated at ATR sites, is likely to promote rapid dephosphorylation at ATR sites by protein phosphatases such as PP2A.

14-3-3γ directly binds Ser296-phosphorylated Chk1

To elucidate the functional changes of Chk1 because of Ser296 phosphorylation, we first measured the *in vitro* kinase activity of each Myc-Chk1 purified from UV-irradiated or non-treated cells. Between WT and S296A, we observed only marginal differences in the elevation of catalytic activity after UV irradiation (Figure 3A). Together with the previous findings for purified Chk1 protein (Chen *et al*, 2000), our observation suggested that Chk1 autophosphorylation exerts limited effects on catalytic activity.

We next searched for proteins binding to Chk1 in a Ser296 phosphorylation-dependent manner. As shown in Figure 3B, signals for anti-14-3-3γ (characterized in Supplementary Figure S3A) were detected in anti-Chk1 immunoprecipitates from UV-irradiated, but not non-treated cells. The signals were diminished by pre-treatment with UCN-01 (Figure 3B) or Chk1 mutations (S296A and K38M; Figure 3C). To further examine the relationship between Chk1 and 14-3-3, we performed the *in vitro* binding analyses using purified 14-3-3 proteins (Figure 3D) and GST-Chk1. As shown in Figure 3E, 14-3-3 bound to autophosphorylated Chk1 in a subtype-specific manner: γ had the highest affinity among all seven subtypes *in vitro*. GST pull-down assay from cell

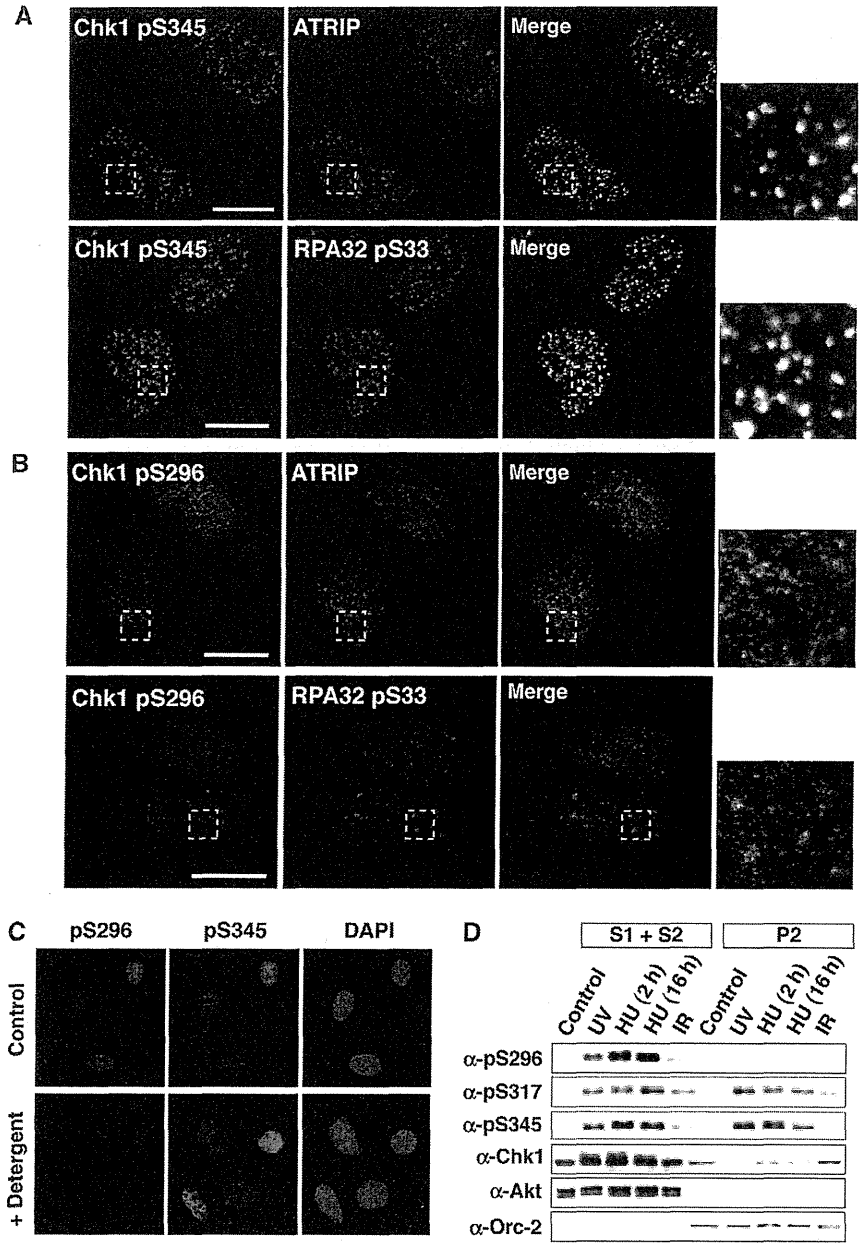

Figure 2 Spatial distributions of phosphorylated Chk1. (**A**, **B**) UV-irradiated HeLa cells were stained with the indicated antibodies. Scale bars are 10 μm. (**C**) UV-irradiated HeLa cells were briefly extracted with Triton X-100 detergent and then stained with the indicated antibodies. (**D**) HeLa cells exposed to UV light or ionizing radiation (IR) or cells treated with hydroxyurea (HU; 2 or 16 h) were fractioned into soluble (S1 + S2) and chromatin (P2) fractions. Akt and Orc-2 were used as markers for soluble and chromatin fractions, respectively.

extracts revealed that K38M or S296A mutants lacked any ability to bind to 14-3-3γ (Supplementary Figure S3B). Although not only γ, but also β and ζ subtypes bound to Chk1 in an UV irradiation-dependent manner, Chk1 binding to β and ζ subtypes was not affected by the pre-treatment with UCN-01 (Supplementary Figure S3C). This observation was consistent with a previous report that β and ζ subtypes bind to Chk1 in a Ser345 phosphorylation-dependent manner (Jiang *et al*, 2003). Thus, all of these results together suggest that Chk1 selects specific subtypes of 14-3-3 in a phosphorylation site-dependent manner and that Ser296 phosphorylation generates binding sites specific for the γ subtype.

Ser296 phosphorylation on Chk1 is essential for DNA damage checkpoint

To examine the significance of Chk1-Ser296 phosphorylation for the DNA damage checkpoint, each Tet-On HeLa cell line was transfected with siRNA specific to Chk1 3′UTR sequence (Figure 4A). One day after transfection, thymidine was added to the growth medium to arrest cells at the G1/S boundary. After incubation with thymidine for 16 h, cells were washed and then incubated with Dox-containing medium to induce each Myc-Chk1 protein or EGFP (mock); we successfully replaced endogenous Chk1 with each exogenous Myc-Chk1 or EGFP (Figure 4B). Six hours after release, cells were

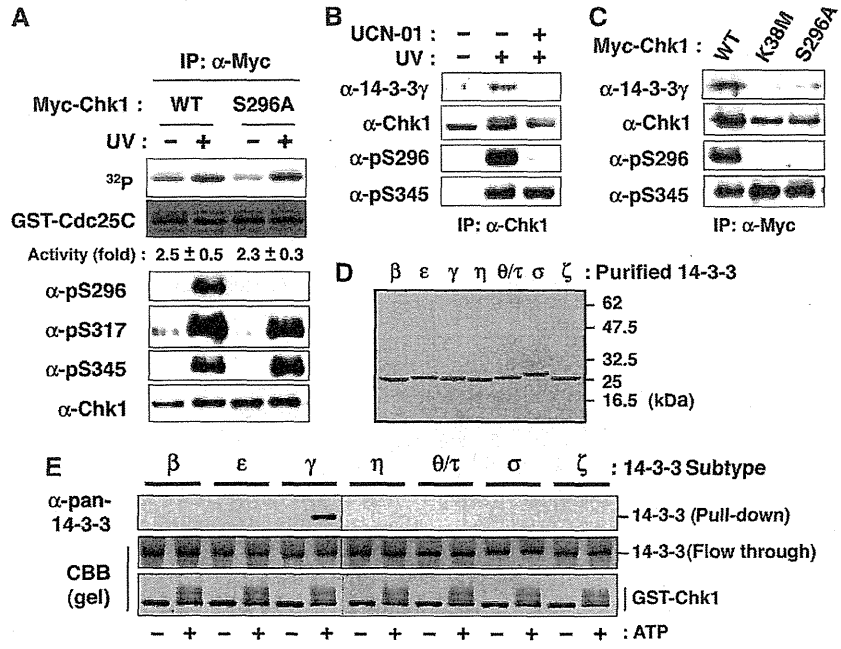

Figure 3 Ser296-phosphorylated Chk1 binds 14-3-3γ. (**A**) *In vitro* kinase activity of individual immunoprecipitated Myc-Chk1 forms (WT or S296A) towards the GST-Cdc25C fragment (195-256 a.a.). Fold activation after UV irradiation is also indicated (mean ± s.e.m. from three independent experiments). (**B**) Detection of endogenous 14-3-3γ in anti-Chk1 immunoprecipitates after UV irradiation. UCN-01 pre-treatment was performed as described in 'Materials and methods'. (**C**) Effects of Chk1 mutation on the complex formation after UV irradiation. Myc-Chk1 WT, K38M or S296A was purified as an anti-Myc immunoprecipitate. (**D**, **E**) GST pull-down assays using GST-Chk1 purified from Sf9 cells and each subtype of 14-3-3 protein purified from bacteria. Each purified 14-3-3 protein was indicated in (**D**). A total of 0.4 μg of GST-Chk1-His was incubated in 20 μl of reaction mixture (25 mM Tris–HCl [pH 7.5], 10 mM $MgCl_2$) with (+) or without (−) 100 μM ATP at 30°C for 60 min. Then, the mixture was rotated with glutathione beads at 4°C. Beads were washed with IP buffer and then rotated with 0.4 μg of each purified 14-3-3 protein in 100 μl of IP buffer at 4°C for 1 h. Beads were then washed and subjected to immunoblotting with anti-pan-14-3-3 (characterized in Supplementary Figure S3A).

irradiated with UV-C light and then incubated in fresh medium containing Dox and nocodazole (to block passage through mitosis) for an additional 6 h. Without UV irradiation, we observed only marginal change in the cumulative mitotic index in these cell lines (Figure 4D; non-irradi.). UV irradiation markedly reduced the cumulative mitotic index in control siRNA-treated cells in which EGFP (mock) was introduced (Figure 4C, compare 'non-irradiated' and 'UV' in 'siControl'). As reported previously (Zhou and Elledge, 2000; Bartek and Lukas, 2003), this DNA damage checkpoint was impaired by reduction of the endogenous Chk1 protein level through the RNA interference mechanism (Figure 4C, compare 'siControl, UV' and 'siChk1-3′UTR UV' in 'mock'). Induction of Myc-Chk1 WT almost nullifies this impairment (Figure 4C and D). However, in contrast, S296A induction hardly rescued checkpoint-deficient cells (Figure 4C and D): we obtained similar results on adding Dox 1 day before thymidine addition (Supplementary Figure S4). In support, we detected higher kinase activity of Cyclin B1/Cdk1 in cells replaced with S296A than with WT (Figure 4E). Our data suggest that Ser296 phosphorylation has critical functions in the DNA damage checkpoint.

14-3-3γ mediates interaction between Chk1 and Cdc25A

How does Ser296 phosphorylation participate in signalling for the DNA damage checkpoint? Higher Cdk1 activity in S296A-replaced cells (Figure 4E) provides some clues. Cdk1 is activated through dephosphorylation of Cdk1-Tyr15 (an inhibitory phosphorylation site) by Cdc25 family phosphatases (Jackman and Pines, 1997), which Chk1 phosphorylates to inhibit their contribution to the DNA damage checkpoint (Sanchez *et al*, 1997; Mailand *et al*, 2000; Zhou and Elledge, 2000; Bartek and Lukas, 2003; Jin *et al*, 2003; Busino *et al*, 2004). Among the phosphatases, we focused on Cdc25A because it appeared to be most affected by UV irradiation in HeLa cells; UV irradiation-induced Cdc25A degradation in a proteasome-dependent manner (Figure 5A) as reported previously (Mailand *et al*, 2000; Busino *et al*, 2004). As shown in Figure 5B, replacement with S296A, but not with WT, caused inhibition of UV damage-dependent Cdc25A degradation, which promoted Cdk1-Tyr15 dephosphorylation. These results suggest that Ser296 phosphorylation is required for Cdc25A degradation.

As Ser296-phosphorylated Chk1 bound to 14-3-3γ (Figure 3; Supplementary Figure S3), we examined whether 14-3-3γ participates in the Cdc25A degradation pathway. As shown in Figure 5C, the transfection with 14-3-3γ-specific siRNA (#1 or #2), but not with control siRNA (cont.) inhibited Cdc25A degradation after UV irradiation, suggesting that 14-3-3γ mediated Cdc25A degradation. GST pull-down assays revealed that 14-3-3γ bound not only Chk1, but also Cdc25A, in UV-irradiated cells (Figure 5D). The pre-treatment with UCN-01 impaired not only Cdc25A degradation, but also 14-3-3γ binding to Chk1 or Cdc25A (Figure 5D). Immunoprecipitation analyses also showed that not only 14-3-3γ but also Cdc25A bound to Myc-Chk1 WT in UV-irradiated cells (Figure 5E and F). This Cdc25A binding to Chk1 was diminished by the S296A mutation (Figure 5E) or 14-3-3γ depletion (Figure 5F). As 14-3-3 proteins form a dimer (Liu *et al*, 1995; Mohammad and Yaffe, 2009), we

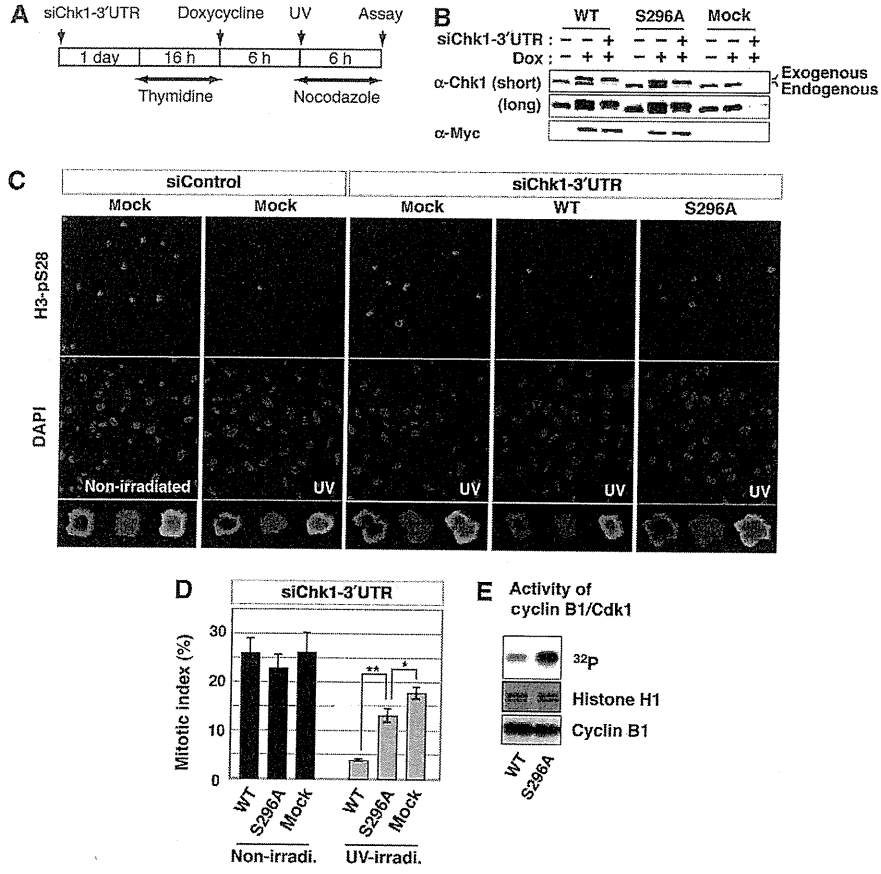

Figure 4 Requirement of Ser296 phosphorylation for Chk1-induced DNA damage checkpoint. (**A**) Scheme of experimental procedures for evaluation of the DNA damage checkpoint. (**B**) Replacement of endogenous Chk1 with each Myc-Chk1 or EGFP (mock) was assessed by immunoblotting with anti-Myc and anti-Chk1 antibodies. (**C**, **D**) Evaluation of mitotic entry after UV irradiation. For calculation of mitotic indices, cells were stained with anti-H3-pSer28 (as a mitotic marker; **C**). Higher magnification image of a mitotic cell in each group is also indicated (**C**, in last row). The graph (**D**) shows the cumulative mitotic index (%) in UV-irradiated or non-irradiated cells in which endogenous Chk1 was replaced with Myc-Chk1 (WT or S296A) or EGFP (mock). Data are mean ± s.e.m. values from three independent experiments ($^{**}P<0.01$, $0.01<{}^{*}P<0.05$). (**E**) H1 kinase activity of Cyclin B1/Cdk1 complex immunoprecipitated from UV-irradiated cells in which endogenous Chk1 was replaced with different Myc-Chk1 forms.

examined whether the dimerization of 14-3-3γ is required for the complex formation between Chk1 and Cdc25A. For this assay, we constructed the dimerization-defective GFP-14-3-3γ mutant (GFP-14-3-3γ DM; Supplementary Figure S5) (Liu *et al*, 1995), which did not lose the ability to bind target phosphoprotein(s) because it bound to Chk1 after UV irradiation (Figure 5G). Although the expression of GFP-14-3-3γ WT recovered the complex formation between Chk1 and Cdc25A in endogenous 14-3-3γ-depleted cells, the induction of GFP-14-3-3γ DM did not rescue it (Figure 5G). To show direct interaction among three proteins, we performed the *in vitro* binding assay using each purified protein. As shown in Figure 5H, GST-Chk1 formed a complex with Cdc25A in a 14-3-3γ-dependent and autophosphorylation-dependent manner. All these results suggest that 14-3-3γ serves as a platform for complex formation between Chk1 and Cdc25A.

Ternary complex formation facilitates Cdc25A-Ser76 phosphorylation by Chk1, which promotes Cdc25A degradation in a βTrCP-dependent manner

Chk1 is known to phosphorylate Cdc25A at multiple sites after DNA damage (Chen *et al*, 2003; Jin *et al*, 2003; Busino *et al*, 2004). Cdc25A-Ser76 is a rate-limiting phosphorylation site for the generation of a βTrCP recognition motif (phosphodegron) by NEK11 (Jin *et al*, 2003; Busino *et al*, 2004; Melixetian *et al*, 2009), although Thr507 phosphorylation creates a docking site for 14-3-3 (Chen *et al*, 2003). We used three strategies to elucidate the effect of Chk1-Ser296 phosphorylation or 14-3-3γ on UV-irradiation-induced Cdc25A phosphorylation/polyubiquitylation (also see Supplementary Figure S6). First, cells were transfected with control or Chk1-3′UTR-specific siRNA and then with Flag-Cdc25A in addition to Myc-Chk1 WT or S296A before UV irradiation. As we observed only marginal changes between mock- and Chk1-depleted cells after UV irradiation (Figure 6A), endogenous Chk1 was unlikely to affect both Flag-Cdc25A phosphorylation and polyubiquitylation in this experimental system. Immunoprecipitation analyses revealed that Flag-Cdc25A was phosphorylated both at Ser76 and Thr507 in cells in which Myc-Chk1 WT was introduced (Figure 6A). However, S296A induction impaired Flag-Cdc25A phosphorylation at Ser76, but not at Thr507 (Figure 6A). S296A expression also reduced Cdc25A polyubiquitylation, compared with the WT case (Figure 6A). Second, cells were transfected with control (−) or 14-3-3γ-specific (+) siRNA and then with Flag-Cdc25A and Myc-Chk1 WT before

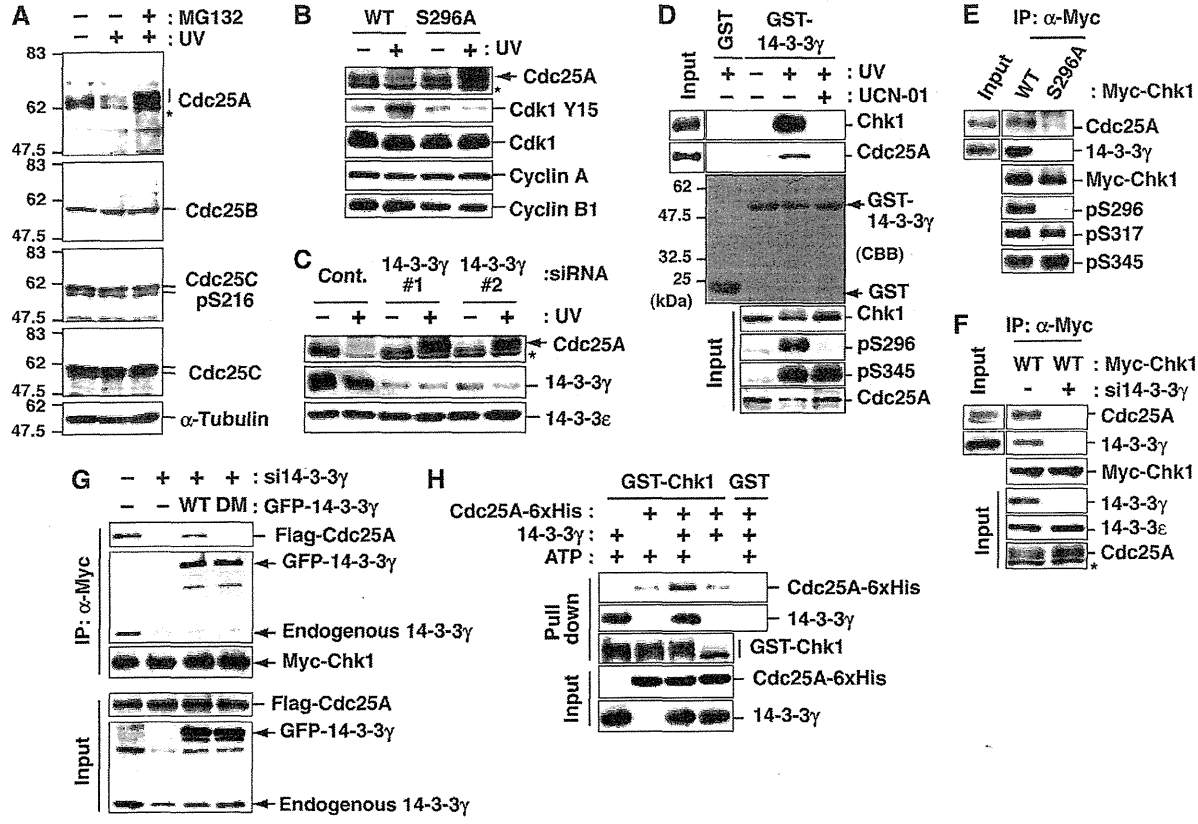

Figure 5 14-3-3γ mediates the interaction between Chk1 and Cdc25A. (**A**) Changes in protein level of each Cdc25 phosphatase or Cdc25C-Ser216 phosphorylation level after UV irradiation. In the last lane, cells were also treated with MG132 from 30 min before UV irradiation to inhibit the proteasome-dependent degradation. (**B**, **C**) Effects of Chk1 mutation (**B**) or 14-3-3γ depletion (**C**) on Cdc25A degradation after UV irradiation. Replacement of endogenous Chk1 with exogenous Myc-tagged Chk1 (**B**; also see Figure 4B) or siRNA treatment of HeLa cells (**C**) was performed as described in 'Materials and methods'. Each cell extract was proved with the indicated antibodies. Asterisks indicate non-specific bands of anti-Cdc25A. (**D**) GST pull-down assays using GST-14-3-3γ. Cells were irradiated with UV and further cultured for 10 min. In the last lane, cells were also treated with UCN-01 from 30 min before UV irradiation. (**E**, **F**) Effects of Chk1 mutation (**E**) or 14-3-3γ knock down (**F**) on ternary complex formation. After Myc-Chk1 induction, cells were irradiated with UV light in the presence of MG132. In panel **F**, cells were transfected with control (−) or 14-3-3γ (#1; +) siRNA at 48 h before UV irradiation. Each anti-Myc immunoprecipitate or cell extract (input) was subjected to the immunoblotting. (**G**) Effect of 14-3-3γ dimerization on the complex formation between Chk1 and Cdc25A. Two days before UV irradiation, cells were transfected with control (−) or 14-3-3γ (#1; +) siRNA. At 1 day before UV irradiation, cells were also transfected with or without (−) GFP-14-3-3γ WT or a dimerization-defective mutant (DM) in addition to Myc-Chk1 WT and Flag-Cdc25A. Cells were irradiated with UV light in the presence of MG132, and then subjected to the immunoprecipitation with an anti-Myc antibody. (**H**) The ternary complex formation among autophosphorylated Chk1, 14-3-3γ and Cdc25A in a purified system. A total of 10 μg of GST-Chk1-His (purified from Sf9 cells) in the presence of 25 μg of 14-3-3γ and/or 25 μg of Cdc25A-6xHis-Myc were incubated in 250 μl of the buffer (25 mM Tris–HCl [pH 7.5], 10 mM $MgCl_2$) with or without 100 μM ATP at 30°C for 1 h. As a negative control, we used 10 μg of GST with the same amounts of 14-3-3γ and Cdc25A-6xHis-Myc. After the incubation, the mixture was rotated with glutathione beads. After washing with IP buffer three times, beads were subjected to immunoblotting.

UV irradiation. As shown in Figure 6B, 14-3-3γ depletion abolished Cdc25A-Ser76 phosphorylation and Cdc25A polyubiquitylation in WT-expressing cells. Finally, cells were transfected with control (−) or 14-3-3γ-specific (+) siRNA and then with Flag-Cdc25A and HA-tagged ubiquitin before UV irradiation. The 14-3-3γ-depletion decreased Flag-Cdc25A polyubiquitylation even in the absence of Myc-Chk1 expression (Figure 6C). Thus, these results indicated that the complex formation between Chk1 and Cdc25A on 14-3-3γ accelerates Cdc25A-Ser76 phosphorylation, which was critical for βTrCP-dependent Cdc25A polyubiquitylation/degradation (Jin *et al*, 2003; Busino *et al*, 2004; Melixetian *et al*, 2009).

To show the importance of 14-3-3γ in Cdc25A-Ser76 phosphorylation more clearly, we performed an *in vitro* assay. In the absence of 14-3-3γ, Chk1 appeared to phosphorylate Cdc25A-Thr507 more effectively than Cdc25A-Ser76 (Figure 6D). Cdc25A-Thr507 phosphorylation depended on the amount of Chk1 protein (Figure 6E) rather than the presence of 14-3-3γ (Figure 6D). On the other hand, Cdc25A-Ser76 appeared to be well correlated with the amount of 14-3-3γ (Figure 6D) rather than that of Chk1 protein (Figure 6E). The Ser296A mutation abolished Cdc25A-Ser76 phosphorylation by Chk1 even in the presence of 14-3-3γ (Figure 6D, see S296A lanes). Similar to Cdc25A-Thr507 phosphorylation, Cdc25C-Ser216 phosphorylation depended on the amount of Chk1 protein rather than that of 14-3-3γ (Figure 6F), suggesting that the 14-3-3γ requirement was relatively specific to Cdc25A-Ser76 phosphorylation. All these observations suggest that 14-3-3γ has a critical function in Cdc25A degradation through the complex formation of Chk1 and Cdc25A on 14-3-3γ during DNA damage.

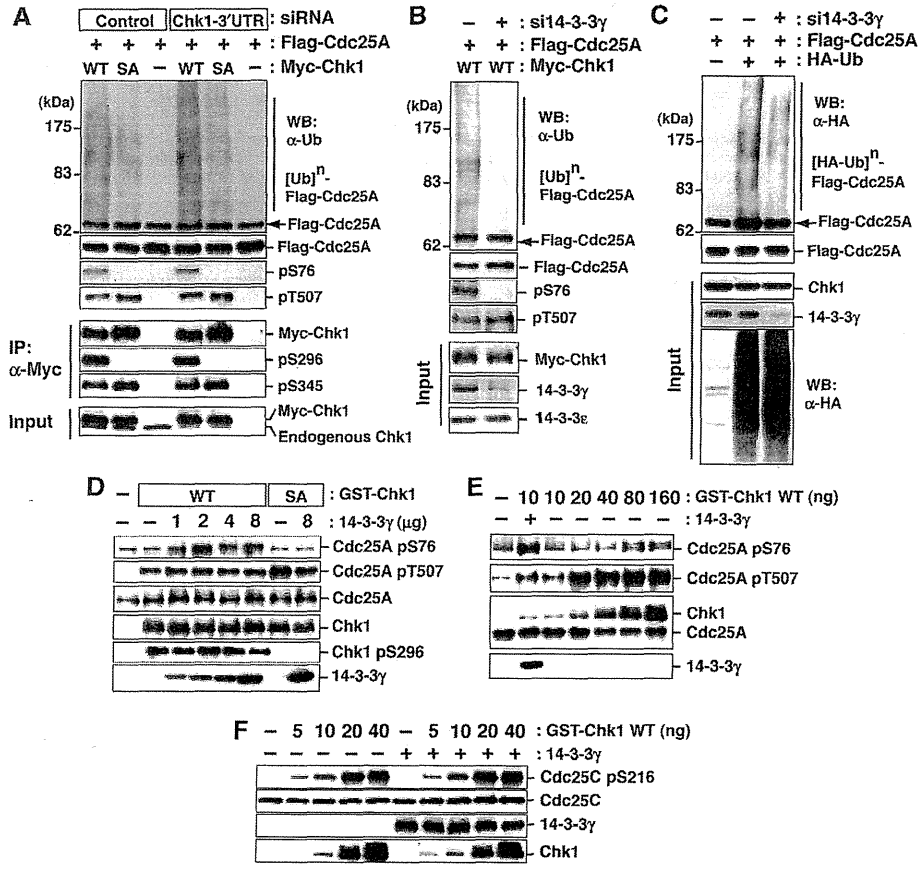

Figure 6 The 14-3-3γ facilitates Chk1 access to Cdc25A-Ser76. (**A–C**) Effects of Chk1 mutation (**A**) or 14-3-3γ knock down (**B**, **C**) on Cdc25A phosphorylation and polyubiquitylation after UV irradiation. Experiments were performed as described in Supplementary Figure S6. Some aliquots of cell extracts were also subjected to the immunoprecipitation with anti-Myc (IP, α-Myc; **A**) or the immunoblotting with the indicated antibodies (Input; **A–C**). (**D**) A total of 1 μg of Cdc25A was incubated with 10 ng of GST-Chk1 (WT or S296A) with or without 14-3-3γ (0–8 μg) in 20 μl of reaction mixture (25 mM Tris–HCl [pH 7.5], 10 mM $MgCl_2$, 100 μM ATP) at 30°C for 5 min. (**E**) In total, 1 μg of Cdc25A was incubated with 10–160 ng of GST-Chk1 (WT) with or without 14-3-3γ (2 μg) in 20 μl of the above mixture at 30°C for 5 min. (**F**) In total, 1 μg of Cdc25C was incubated with 0–40 ng of GST-Chk1 (WT) with or without 14-3-3γ (2 μg) in 20 μl of the above mixture at 30°C for 5 min.

Discussion

A long-standing concept in the functions of mammalian 14-3-3 during DNA damage has been that 14-3-3 binds Cdc25C phosphorylated at Ser216 by Chk1 and negatively regulates Cdc25C activity. The 14-3-3-binding sequence including a phosphorylation site (Ser216 on human Cdc25C) is conserved from yeast to mammals, and Chk1 phosphorylates Cdc25C at Ser216 in mammalian cells (Furnari *et al*, 1997; Peng *et al*, 1997; Sanchez *et al*, 1997; Pines, 1999). Thus, mammalian 14-3-3 proteins have long been believed to modulate the checkpoint signal from Chk1 to Cdc25C. However, Cdc25C-Ser216 is highly phosphorylated (probably by C-TAK1) throughout interphase in the absence of DNA damage (Peng *et al*, 1998; Russell, 1998; Zhou and Elledge, 2000): we obtained a similar result (Figure 5A). Cdc25B is also reported to be phosphorylated in the absence of DNA damage (Schmitt *et al*, 2006). Genetic studies raised similar question of whether Chk1 and 14-3-3 proteins act through Cdc25C (or Cdc25B) in the checkpoint response, because normal cell cycle progression and checkpoint responses were observed in mice and cells lacking Cdc25B and Cdc25C (Chen *et al*, 2001; Lincoln *et al*, 2002; Ferguson *et al*, 2005). In sharp contrast, Cdc25A null (−/−) mice die on embryonic day 5–7 during the peri-implantation period (Ray and Kiyokawa, 2007; Ray *et al*, 2007), suggesting the possibility that Cdc25A may be the most effective Cdk activator during cell cycle progression. Here, we report that 14-3-3 binds Chk1 autophosphorylated at Ser296 in a γ-subtype-specific manner. The complex formation of Chk1 and Cdc25A on 14-3-3γ facilitates Cdc25A phosphorylation at Ser76, a critical phosphorylation site for degradation (Jin *et al*, 2003; Busino *et al*, 2004; Melixetian *et al*, 2009).

Our model is summarized in Figure 7. At sites (foci) where DNA damage occurs, ATR is first activated and then phosphorylates Ser317 and Ser345 on Chk1. This ATR-induced Chk1 phosphorylation stimulates the catalytic activity of Chk1, resulting in autophosphorylation at Ser296, which generates a docking site for 14-3-3γ. Chk1 activation is also likely to elevate the level of Cdc25A phosphorylation at Thr507, but not at Ser76. Dimer formation by 14-3-3 proteins facilitates their function as platforms for generation of complexes between Chk1 and Cdc25A. Such ternary complex formation enables Chk1 to phosphorylate Cdc25A at Ser76. This phosphorylation induces the generation of a βTrCP recognition motif (phosphodegron) by NEK11 (Jin *et al*, 2003; Busino *et al*, 2004; Melixetian *et al*, 2009), which results in βTrCP-dependent Cdc25A degradation. This proteasome-dependent

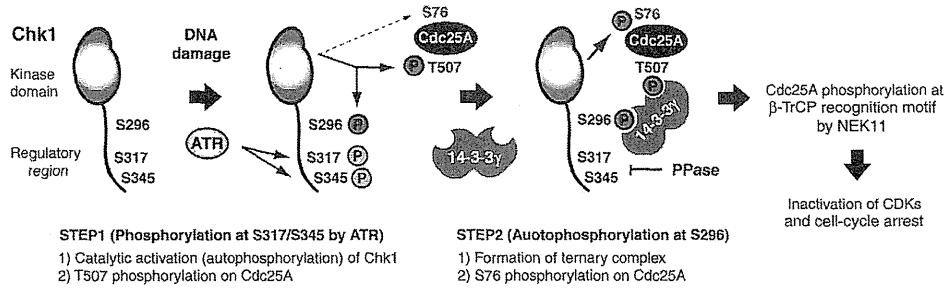

Figure 7 Model for sequential actions of Chk1 after DNA damage.

Cdc25A degradation prevents premature activation of Cdks and induces cell cycle arrest after DNA damage (Zhou and Elledge, 2000; Bartek and Lukas, 2003).

During the checkpoint response, Chk1 is accumulated at the nucleus (Jiang *et al*, 2003), where Cdc25A is enriched. This nuclear accumulation reportedly depends on Chk1-Ser345 phosphorylation (Jiang *et al*, 2003). As Chk1-Ser296 phosphorylation depends on ATR-induced phosphorylation, our observation also raised another possibility that Chk1-Ser296 autophosphorylation and/or 14-3-3γ might have an important function in Chk1 translocation from cytoplasm to nucleus. We examined the subcellular localization of Myc-Chk1 WT or S296A before or after UV irradiation, but found only marginal changes in the nucleus/cytoplasm ratio between the two proteins (data not shown). In addition, 14-3-3γ depletion had little impact on Chk1 localization before or after UV irradiation (data not shown). Hence, nuclear accumulation of Chk1 is likely to be regulated by Chk1-Ser345 phosphorylation rather than Chk1-Ser296 autophosphorylation and 14-3-3γ association.

Our present data thus provide strong evidence that 14-3-3γ mediates Chk1-induced Cdc25A proteolysis through complex formation between Chk1 and Cdc25A. We propose that Chk1 and 14-3-3 act through Cdc25A in the DNA damage checkpoint response. However, checkpoint regulation by 14-3-3 proteins appears to be more complex in mammalian cells. β and ζ subtypes of 14-3-3 also bind Chk1 in a Ser345 phosphorylation-dependent manner (Jiang *et al*, 2003) (see also Supplementary Figure S3C). This binding appears to have different functions in checkpoint signalling, as it promotes the nuclear retention of Chk1 likely through the masking of NES on Chk1 (Jiang *et al*, 2003). Once Ser296 phosphorylation occurs, Ser345 rapidly undergoes dephosphorylation (Leung-Pineda *et al*, 2006). In contrast, Ser296 phosphorylation induces binding to 14-3-3γ, which promotes Cdc25A degradation. Such ordered binding of Chk1 to specific 14-3-3 subtype(s) may indeed have a critical function in checkpoint signalling.

In our *in vitro* assays, Chk1-Ser296 phosphorylation occurred (Figure 1C; Supplementary Figure S1E), although we observed little or no phosphorylation of Chk1 by ATR (Supplementary Figure S1E). Thus, these *in vitro* phenomena appear to contrast with what happens *in vivo*. As the Chk1 C-terminal regulatory domain was reported to inhibit the catalytic activation of Chk1 (Katsuragi and Sagata, 2004; Walker *et al*, 2009), this contrast may be due to the difference in the way inhibition of the Chk1 C-terminal regulatory domain is cancelled. Under the *in vitro* condition, the detergent treatment was reported to induce the structural change of Chk1 C-terminal regulatory domain, which cancelled C-terminal inhibition and then stimulated the catalytic activity in the absence of ATR-induced phosphorylation (Walker *et al*, 2009). Similar observations were obtained by using Chk1 protein expressed in bacteria. The catalytic activity towards Chk1-Ser296 was elevated by the usage of 1% sarcosyl for bacteria lysis (Figure 1C) (Zhao and Piwnica-Worms, 2001). Therefore, we consider that the C-terminal inhibition is also cancelled during Chk1 purification from insect cells. However, in cells, such cancellation was performed by ATR-induced Chk1 phosphorylation (Zhao and Piwnica-Worms, 2001; Walker *et al*, 2009). Thus, Ser296 autophosphorylation is likely to require pre-phosphorylation at Ser317 and Ser345 in cells.

In this study, we showed the Chk1 autophosphorylation at Ser296 after ATR-induced phosphorylation. Ser296 phosphorylation makes a docking site for 14-3-3 in a γ-subtype-specific manner. Chk1 binding to 14-3-3γ promotes the complex formation between Chk1 and Cdc25A, which induces Cdc25A-Ser76 phosphorylation and then Cdc25A polyubiquitylation/degradation. Our *in vitro* analyses also revealed that Chk1 had several autophosphorylation sites other than Ser296 (Supplementary Figure S1E). In this way, Chk1 autophosphorylation at other site(s) may also have a critical function in checkpoint signalling. Further studies in this regard will be undertaken in future.

Materials and methods

Cell culture

We established HeLa cells in which each type of Myc-tagged Chk1 was expressed in a tetracycline/Dox-dependent manner, as described previously (Ikegami *et al*, 2008). HeLa or Tet-ON HeLa cells were grown in DME medium supplemented with 10% FBS. For Myc-Chk1 induction, Tet-ON HeLa cells were treated with 0.1–1.0 μg/ml of Dox (Sigma, St Louis, MO) for 1 day, except in the case illustrated in Figure 4.

For inhibitor experiments, cells were pre-treated with or without 300 nM UCN-01 (a Chk1 inhibitor; Merck, Whitehouse Station, NJ) or 20 mM caffeine (an ATR and ATM inhibitor; Wako Pure Chemical, Osaka, Japan) in the presence or absence of 10 μM MG132 (Merck) for 30 min. After culture medium was removed, cells in uncovered tissue culture dishes were treated with or without 254-nm UV light at a dose of 5 or 10 J/m^2 (FUNA-UV-LINKER, Funakoshi, Tokyo, Japan). The same medium was re-added back and incubated for an additional 10 (Figure 5D), 30 (Figures 5A–C, E–G, and 6A–C) or 60 min (Ikegami *et al*, 2008). Biochemical fractionation was performed as reported (Jiang *et al*, 2003; Smits *et al*, 2006).

For immunocytochemistry, cells grown on coverslips were fixed with 2% formaldehyde for 20 min and then permeabilized with 0.1% Triton X-100 in phosphate-buffered saline at room temperature.

Transfection

siRNA duplexes were purchased from Qiagen (Valencia, CA). Target sequences were as follows: a negative control, AATTCTCCG AACGTGTCACGT; Chk1, AAGGTGAATATAGTGCTGCTA (3′UTR); 14-3-3γ, AAGAGCTATATCCTTAACCAT (#1) and CACTGTCGAATG AGGAACGAA (#2). Transfection was performed with mixtures of each siRNA (final concentration, 20 nM) and Lipofectamine™ RNAiMAX reagent, according to the reverse transfection procedures (Invitrogen, Carlsbad, CA).

Human Cdc25A or myc-Chk1 DNA was inserted into pCMV-Tag2B (Stratagene, La Jolla, CA) or pIRES-Puro3 (Clontech, Mountain View, CA), respectively. pEGFP-C1-14-3-3 or pCGN-HA-ubiquitin was kindly provided by Dr Kaibuchi (Nagoya University) or Dr Kikuchi (Osaka University). We constructed the dimerization-defective 14-3-3γ mutant (GFP-14-3-3γ DM) using site-directed mutagenesis: 14-3-3γ was mutated at Glu5 to Lys (E5K), at Leu12 to Gln (L12Q), at Ala13 to Gln (A13Q), at Glu14 to Arg (E14R), at Tyr85 to Gln (Y85Q), at Lys88 to Asn (K88N) and at Glu89 to Gln (E89Q) as described previously (Liu *et al*, 1995). Plasmid transfection was performed with *Trans*IT-LT1® according to the manufacturers' protocol (Mirus, Madison, WI).

Antibodies

We produced site- and phosphorylation state-specific antibodies for Ser28 on histone H3 and Ser296, Ser317 and Ser345 (Ikegami *et al*, 2008) on Chk1 (rat monoclonal antibodies), as described previously (Goto and Inagaki, 2007). Competition experiments using peptides (Figure 1B) were also performed as detailed earlier (Sekimata *et al*, 1996). Antibodies from commercial sources were as follows: mouse anti-Chk1 (G4), anti-14-3-3ε (8C3), anti-pan-14-3-3 (H-8), anti-Cyclin B1 (GNS-1), anti-GST (B-14), anti-His (H-3) and rabbit anti-14-3-3γ (C-16) from Santa Cruz Biotechnology (Santa Cruz, CA); rabbit anti-Chk1-pSer317 and -pSer345 (133D3), anti-Akt, anti-Cdc25C (5H9) and anti-Cdc25C pSer216 (63F9) from Cell Signaling Technology (Beverly, MA); mouse anti-Cdc25A (DCS-120 + DCS-121), rabbit anti-Cdc25A pSer75 and anti-ATRIP from Abcam (Cambridge, UK); mouse anti-Cyclin A, -Cdc25B, -Cdk1, -Cdk1 pTyr15 and -Orc-2 from BD Biosciences (San Jose, CA); mouse anti-Chk1 (DCS-310) and -α-tubulin (B-5-12) from Sigma; rabbit anti-RPA32 pSer33 (BL744) from Benthyl Laboratories (Montgomery, TX); rabbit anti-Cdc25A pThr506 from ABGENT (San Diego, CA); mouse anti-Myc (4A6) from Millipore (Bedford, MA), mouse anti-HA (12CA5) and anti-GFP (clone 7.1 and 13.1) from Roche Diagnostics (Mannheim, Germany); and mouse anti-Ubiquitin (P4G7) from COVANCE (Berkeley, CA).

Evaluation of mitotic entry

Each Tet-On HeLa cell line was transfected with siRNA for Chk1-3′UTR sequence according to the reverse transfection protocol (Invitrogen). One day after the transfection, we added 2 mM thymidine to the growth medium. After incubation with thymidine for 16 h, cells were extensively washed with pre-warmed PBS and then incubated with Dox-containing medium. Six hours after release, cells were irradiated with UV (5 J/m^2) and then incubated in fresh medium containing Dox and 0.1 μg/ml nocodazole (to block passage through mitosis) for an additional 6 h. For the calculation of mitotic indices, cells were fixed and then stained with anti-H3-pSer28 as a mitotic marker (Goto *et al*, 1999). We judged mitotic cells not only by morphological features of nuclei or chromosomes (DAPI-staining patterns), but also by the detection of mitotic H3-Ser28 phosphorylation in chromosomes.

Protein purification

For bacterial expression of GST-tagged 14-3-3 and Cdc25C fragment (residues 195–256), *Escherichia coli* strain DH5α (Invitrogen) was transformed with pGEX-6P-1 (GE Healthcare, Little Chalfont, Buckinghamshire, UK) carrying each protein. Each GST-fusion protein was expressed in the presence of 0.2 mM IPTG at 30°C for 4 h. Each protein was purified through glutathione chromatography (GE Healthcare).

GST-Chk1-His (WT, S296A or K38M), Cdc25A-6xHis-Myc or Cdc25C-6xHis-HA was expressed in Sf9 cells for 3 days. After the manufacturers' protocol (GE Healthcare or Qiagen), GST-tagged or His-tagged protein was purified through glutathione- or nickel-affinity chromatography, with slight modifications. As proteins purified from Sf9 cells were already phosphorylated at several sites (data not shown), these proteins attached on the beads were treated with λ protein phosphatase (λPPase; Cell Signaling Technology) at 30°C for 1 h. After washing of the beads, recombinant proteins were eluted according to each protocol.

In some experiments, GST was removed from GST-14-3-3 (Figures 3D, E, 5H, and 6D–F) and GST-Chk1-His (Supplementary Figure 1E) through cleavage at the linker region by PreScission Protease (GE Healthcare) and then absorbed onto the glutathione beads.

Immunoprecipitation and GST pull-down assays from cell extracts

Cells were lysed in IP buffer (50 mM Tris–HCl [pH 7.5], 0.1 M NaCl, 50 mM β-glycerophosphate, 50 mM NaF, 1 mM Na_3VO_4, 50 mM sodium pyrophosphate, 2 mM EDTA, 1 mM EGTA, 1% NP-40 and 1 mM PMSF) at 4°C. After centrifugation (17 000 *g*) for 15 min at 4°C, the supernatant was subjected to immunoprecipitation (Ikegami *et al*, 2008) or GST pull-down assays. For the latter, supernatant was incubated with GST-fusion protein at 4°C for 2 h. After centrifugation (170 000 *g*) for 15 min at 4°C, the mixture was incubated with glutathione beads for 30 min at 4°C with rotation. The beads were then washed with IP buffer twice and subjected to immunoblotting. We used appropriate HRP-conjugated, light chain-specific antibodies (Jackson ImmunoResearch Laboratories, Inc., West Grove, PA) for the detection of immunoprecipitated Chk1.

In vitro kinase assays

For measurement of Myc-Chk1 kinase activity (Figure 3A), each Myc-Chk1 protein was purified as an anti-Myc immunoprecipitate (Ikegami *et al*, 2008) from 5×10^6 cells and incubated with 5 μg of GST-Cdc25C fragment (195–256 a.a.) in 20 μl of buffer (25 mM Tris–HCl [pH 7.5], 10 mM $MgCl_2$ and 10 mM [γ-^{32}P] ATP [10 μCi]) at 30°C for 30 min. For measurement of cyclin B1/Cdk1 kinase activity (Figure 4E), cyclin B1/Cdk1 complexes were purified with anti-Cyclin B1 (Ikegami *et al*, 2008) from 2×10^5 cells and incubated with 4 μg of histone H1 (Roche Diagnostics) in 20 μl of reaction buffer (25 mM Tris–HCl [pH 7.5], 10 mM $MgCl_2$ and 100 μM [γ-^{32}P] ATP [1 μCi]) at 30°C for 5 min.

In vivo ubiquitylation assays

Cells were lysed in hot buffer (95°C) containing 25 mM Tris–HCl (pH 8.0), 1.5% SDS, 0.15% sodium deoxycholate, 0.15% NP-40, 1 mM EDTA, 1 μM okadaic acid and 5 mM N-ethylmaleimide. The lysates were diluted (1:10) with NP-40 lysis buffer (50 mM Hepes at pH 7.4, 150 mM NaCl, 1 mM EDTA, 1 mM EGTA and 0.15% NP-40) and used for immunoprecipitation of Flag-Cdc25A with Anti-FLAG M2 affinity gel (Sigma). Immunoprecipitates were washed three times with NP-40 lysis buffer supplemented with 1 M NaCl and then analysed by SDS–PAGE.

Supplementary data

Supplementary data are available at *The EMBO Journal* Online (http://www.embojournal.org).

Acknowledgements

We thank K Kaibuchi (Nagoya University) for providing human 14-3-3 cDNAs, A Kikuchi (Osaka University) for pCGN-HA-ubiquitin, M Nakanishi (Nagoya City University) for a baculovirus carrying Chk1 and a DNA construct for GST-Cdc25C fragment expression and K Yamashita (Kanazawa University) for baculoviruses carrying Cdc25A and Cdc25C. We are indebted to M Matsuyama for performing the experiments in Figure 1C and Y Ikegami (Nagoya City University), Y Hayashi, C Yuhara and K Kobori for technical assistance. We are grateful to Y Takada for secretarial expertise, and M Moore and J Shields for critical comments on the paper. This work was supported in part by Grants-in-Aid for Scientific Research from the Japan Society for the Promotion of Science and from the Ministry of Education, Science, Technology, Sports and Culture of Japan; by a Grant-in-Aid for the Third-Term Comprehensive 10-Year Strategy for Cancer Control from the Ministry of Health and Welfare, Japan; by the Uehara Memorial Foundation; the Naito Foundation; the Takeda Science Foundation and a Research Grant from the Princess Takamatsu Cancer Research Fund.

Conflict of interest

The authors declare that they have no conflict of interest.

References

Bartek J, Lukas J (2003) Chk1 and Chk2 kinases in checkpoint control and cancer. *Cancer Cell* **3:** 421–429

Boutros R, Lobjois V, Ducommun B (2007) CDC25 phosphatases in cancer cells: key players? Good targets? *Nat Rev Cancer* **7:** 495–507

Busino L, Chiesa M, Draetta GF, Donzelli M (2004) Cdc25A phosphatase: combinatorial phosphorylation, ubiquitylation and proteolysis. *Oncogene* **23:** 2050–2056

Busino L, Donzelli M, Chiesa M, Guardavaccaro D, Ganoth D, Dorrello NV, Hershko A, Pagano M, Draetta GF (2003) Degradation of Cdc25A by beta-TrCP during S phase and in response to DNA damage. *Nature* **426:** 87–91

Chen MS, Hurov J, White LS, Woodford-Thomas T, Piwnica-Worms H (2001) Absence of apparent phenotype in mice lacking Cdc25C protein phosphatase. *Mol Cell Biol* **21:** 3853–3861

Chen MS, Ryan CE, Piwnica-Worms H (2003) Chk1 kinase negatively regulates mitotic function of Cdc25A phosphatase through 14-3-3 binding. *Mol Cell Biol* **23:** 7488–7497

Chen P, Luo C, Deng Y, Ryan K, Register J, Margosiak S, Tempczyk-Russell A, Nguyen B, Myers P, Lundgren K, Kan CC, O'Connor PM (2000) The 1.7 A crystal structure of human cell cycle checkpoint kinase Chk1: implications for Chk1 regulation. *Cell* **100:** 681–692

Clarke CA, Clarke PR (2005) DNA-dependent phosphorylation of Chk1 and Claspin in a human cell-free system. *Biochem J* **388:** 705–712

Dunaway S, Liu HY, Walworth NC (2005) Interaction of 14-3-3 protein with Chk1 affects localization and checkpoint function. *J Cell Sci* **118:** 39–50

Ferguson AM, White LS, Donovan PJ, Piwnica-Worms H (2005) Normal cell cycle and checkpoint responses in mice and cells lacking Cdc25B and Cdc25C protein phosphatases. *Mol Cell Biol* **25:** 2853–2860

Ford JC, al-Khodairy F, Fotou E, Sheldrick KS, Griffiths DJ, Carr AM (1994) 14-3-3 protein homologs required for the DNA damage checkpoint in fission yeast. *Science* **265:** 533–535

Furnari B, Rhind N, Russell P (1997) Cdc25 mitotic inducer targeted by chk1 DNA damage checkpoint kinase. *Science* **277:** 1495–1497

Goto H, Inagaki M (2007) Production of a site- and phosphorylation state-specific antibody. *Nat Protoc* **2:** 2574–2581

Goto H, Tomono Y, Ajiro K, Kosako H, Fujita M, Sakurai M, Okawa K, Iwamatsu A, Okigaki T, Takahashi T, Inagaki M (1999) Identification of a novel phosphorylation site on histone H3 coupled with mitotic chromosome condensation. *J Biol Chem* **274:** 25543–25549

Ikegami Y, Goto H, Kiyono T, Enomoto M, Kasahara K, Tomono Y, Tozawa K, Morita A, Kohri K, Inagaki M (2008) Chk1 phosphorylation at Ser286 and Ser301 occurs with both stalled DNA replication and damage checkpoint stimulation. *Biochem Biophys Res Commun* **377:** 1227–1231

Jackman MR, Pines JN (1997) Cyclins and the G2/M transition. *Cancer Surv* **29:** 47–73

Jiang K, Pereira E, Maxfield M, Russell B, Goudelock DM, Sanchez Y (2003) Regulation of Chk1 includes chromatin association and 14-3-3 binding following phosphorylation on Ser-345. *J Biol Chem* **278:** 25207–25217

Jin J, Shirogane T, Xu L, Nalepa G, Qin J, Elledge SJ, Harper JW (2003) SCFbeta-TRCP links Chk1 signaling to degradation of the Cdc25A protein phosphatase. *Genes Dev* **17:** 3062–3074

Kastan MB, Bartek J (2004) Cell-cycle checkpoints and cancer. *Nature* **432:** 316–323

Katsuragi Y, Sagata N (2004) Regulation of Chk1 kinase by autoinhibition and ATR-mediated phosphorylation. *Mol Biol Cell* **15:** 1680–1689

Leung-Pineda V, Ryan CE, Piwnica-Worms H (2006) Phosphorylation of Chk1 by ATR is antagonized by a Chk1-regulated protein phosphatase 2A circuit. *Mol Cell Biol* **26:** 7529–7538

Lincoln AJ, Wickramasinghe D, Stein P, Schultz RM, Palko ME, De Miguel MP, Tessarollo L, Donovan PJ (2002) Cdc25b phosphatase is required for resumption of meiosis during oocyte maturation. *Nat Genet* **30:** 446–449

Liu D, Bienkowska J, Petosa C, Collier RJ, Fu H, Liddington R (1995) Crystal structure of the zeta isoform of the 14-3-3 protein. *Nature* **376:** 191–194

Mailand N, Falck J, Lukas C, Syljuasen RG, Welcker M, Bartek J, Lukas J (2000) Rapid destruction of human Cdc25A in response to DNA damage. *Science* **288:** 1425–1429

Melixetian M, Klein DK, Sorensen CS, Helin K (2009) NEK11 regulates CDC25A degradation and the IR-induced G2/M checkpoint. *Nat Cell Biol* **11:** 1247–1253

Mohammad DH, Yaffe MB (2009) 14-3-3 proteins, FHA domains and BRCT domains in the DNA damage response. *DNA Repair (Amst)* **8:** 1009–1017

Neely KE, Piwnica-Worms H (2003) Cdc25A regulation: to destroy or not to destroy—is that the only question? *Cell Cycle* **2:** 455–457

Peng CY, Graves PR, Ogg S, Thoma RS, Byrnes III MJ, Wu Z, Stephenson MT, Piwnica-Worms H (1998) C-TAK1 protein kinase phosphorylates human Cdc25C on serine 216 and promotes 14-3-3 protein binding. *Cell Growth Differ* **9:** 197–208

Peng CY, Graves PR, Thoma RS, Wu Z, Shaw AS, Piwnica-Worms H (1997) Mitotic and G2 checkpoint control: regulation of 14-3-3 protein binding by phosphorylation of Cdc25C on serine-216. *Science* **277:** 1501–1505

Pines J (1999) Cell cycle. Checkpoint on the nuclear frontier. *Nature* **397:** 104–105

Puc J, Keniry M, Li HS, Pandita TK, Choudhury AD, Memeo L, Mansukhani M, Murty VV, Gaciong Z, Meek SE, Piwnica-Worms H, Hibshoosh H, Parsons R (2005) Lack of PTEN sequesters CHK1 and initiates genetic instability. *Cancer Cell* **7:** 193–204

Ray D, Kiyokawa H (2007) CDC25A levels determine the balance of proliferation and checkpoint response. *Cell Cycle* **6:** 3039–3042

Ray D, Terao Y, Nimbalkar D, Hirai H, Osmundson EC, Zou X, Franks R, Christov K, Kiyokawa H (2007) Hemizygous disruption of Cdc25A inhibits cellular transformation and mammary tumorigenesis in mice. *Cancer Res* **67:** 6605–6611

Russell P (1998) Checkpoints on the road to mitosis. *Trends Biochem Sci* **23:** 399–402

Sanchez Y, Wong C, Thoma RS, Richman R, Wu Z, Piwnica-Worms H, Elledge SJ (1997) Conservation of the Chk1 checkpoint pathway in mammals: linkage of DNA damage to Cdk regulation through Cdc25. *Science* **277:** 1497–1501

Schmitt E, Boutros R, Froment C, Monsarrat B, Ducommun B, Dozier C (2006) CHK1 phosphorylates CDC25B during the cell cycle in the absence of DNA damage. *J Cell Sci* **119:** 4269–4275

Sekimata M, Tsujimura K, Tanaka J, Takeuchi Y, Inagaki N, Inagaki M (1996) Detection of protein kinase activity specifically activated at metaphase-anaphase transition. *J Cell Biol* **132:** 635–641

Smits VA, Reaper PM, Jackson SP (2006) Rapid PIKK-dependent release of Chk1 from chromatin promotes the DNA-damage checkpoint response. *Curr Biol* **16:** 150–159

Walker M, Black EJ, Oehler V, Gillespie DA, Scott MT (2009) Chk1 C-terminal regulatory phosphorylation mediates checkpoint activation by de-repression of Chk1 catalytic activity. *Oncogene* **28:** 2314–2323

Zhao H, Piwnica-Worms H (2001) ATR-mediated checkpoint pathways regulate phosphorylation and activation of human Chk1. *Mol Cell Biol* **21:** 4129–4139

Zhou BB, Elledge SJ (2000) The DNA damage response: putting checkpoints in perspective. *Nature* **408:** 433–439

Zou L, Elledge SJ (2003) Sensing DNA damage through ATRIP recognition of RPA-ssDNA complexes. *Science* **300:** 1542–1548